8

From Clay Mineral Crystals to Colloidal Clay Mineral Dispersions

Gerhard Lagaly
Institute of Inorganic Chemistry, University of Kiel, Kiel, Germany

I. INTRODUCTION

Colloid scientists dream of colloidal dispersions to behave as demanded by theories. Probably the dreams can never be realized; neither the systems nor the theories are perfect.

Two systems are sometimes considered ideal: latex and clay dispersions. Latex particles can behave as ideal hydro-

phobic colloids (the DLVO theory describes the properties correctly) but strong deviations are often observed. The reputation of clay mineral dispersions as suitable model systems is based on the fact that the surface structure of these plate-like particles is well known and that minerals with widely differing properties are available. However, clay mineral dispersions never behave as ideal systems. Coagulation and flocculation processes are much more dependent on system parameters than for other dispersions. Several reasons must be mentioned that contribute to this behavior:

1. The particles are of irregular shape and of different thicknesses. The layers composing one particle have no common contour line and are frayed out.
2. The particles are often very thin and possess remarkable flexibility.
3. Particles with narrow size distribution cannot be obtained.
4. The crystals of smectites disarticulate into thinner lamellae or single silicate layers when certain experimental conditions are fulfilled.
5. The charges of the layers are not uniformly distributed.
6. The particles also carry charges at the edges, which change with the chemical parameters, in particular with pH.

Because of these facts, straightforward calculations of stability and coagulation conditions are difficult to obtain. Nevertheless, many practical uses of clay dispersions are just based on the variation of the colloidal stability with the system parameters.

II. CLAY MINERAL STRUCTURE

A. Clays and Clay Minerals

Clays are fine-grained sediments with particle sizes $<2\,\mu m$. The clay minerals are the decisive components in clays. Properties, which are considered typical of clays (plasticity, thixotropy, water retention, swelling, ion exchange, adsorption of

inorganic and organic compounds), are related to the presence of these minerals. Among the indifferent components, quartz should be mentioned first because it is an abundant main component besides the clay minerals. The yellow-brown color of clays is mainly caused by iron oxides. The amount of organic materials in clays is often small but can have a strong influence on color and the colloidal and flow properties.

The most important clay minerals are kaolinite, smectites, illites, and mixed-layer minerals. Clays containing appreciable amounts of kaolinite are called kaolins. Smectites, mostly montmorillonites, are the main constituents in bentonites. Clays are formed by precipitation from fluids, by weathering or hydrothermal alteration of different types of parent minerals and by hydrothermal neoformation.

Bentonites in technical applications are mainly used without further processing as they are fine-grained materials with particles mainly $<2\ \mu m$. They may be transferred into the sodium form (alkaline or soda activation) and into organic derivatives (organic activation) or may be decomposed to bleaching earths (acid activation) [1–3].

Kaolins normally contain coarser particles of quartz, feldspars, micas, unaltered granite, etc., and have to be benefited by size separation or refining (hydrocycloning, sedimentation, flotation, high-gradient magnetic separation) [4].

Common clays are dominant in ceramics, bricks, tiles, and in the building industry including half-timbering and contain kaolinite, illite–sericite, quartz, and illite–smectite mixed-layer materials in very different ratios.

Synthetic clay minerals containing aluminum are difficult to obtain, and colloidal dispersions of these materials are rarely studied. Phases that are similar to hectorite (a magnesium lithium smectite) are more easily obtainable. For instance, Laponite is produced by Laporte Industries on a technical scale, and other companies also expand capacity for the production of similar materials. An advantage of these synthetic clay minerals is the purity and the ease with which they form colloidal dispersions [5–11]. Magnesium lithium silicates can also be prepared from melts [10]. They are often called synthetic fluoro hectorites but their layer charge

can be distinctly higher than for hectorite minerals and Laponite. Na-4-micas with high-Al content were also be prepared by solid-state reactions [10,12]. For other clay minerals, see Ref. [13].

B. Structure of Clay Minerals

The clay minerals considered here are composed of continuous two-dimensional tetrahedral sheets of composition $(Si, Al)_2O_5$ and octahedral sheets which normally contain Mg^{2+}, Al^{3+}, Fe^{2+}, and Fe^{3+} cations (Figure 8.1) [2,14].

When one tetrahedral sheet is linked to one octahedral sheet, the assemblage is known as 1:1 layer silicate (Figure

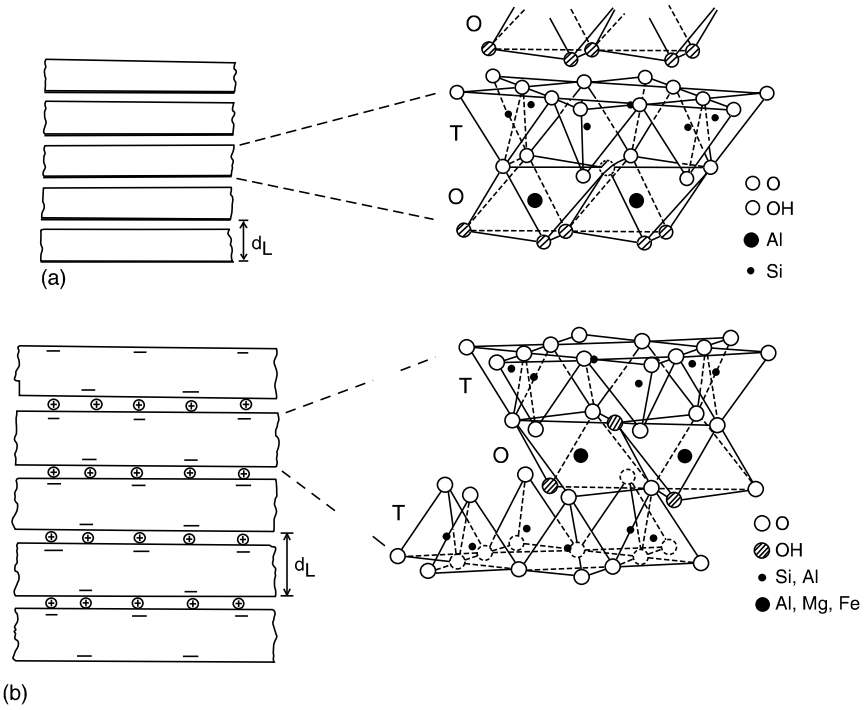

Figure 8.1 Structure of clay minerals. T, tetrahedral sheet; O, octahedral sheet; C, interlayer cations ($+H_2O$). (a) 1:1 clay minerals (kaolinite); (b) 2:1 clay minerals (smectites, vermiculites, micas). (From K. Jasmund and G. Lagaly, Tonminerale und Tone, Figure 1.2. Ref. 2. With permission.)

8.1(a)). The predominant species of this group of minerals is kaolinite. The layers are uncharged and held together by hydrogen bonds and van der Waals interactions. The positions of adjacent layers are governed by the requirement for pairing the OH groups on the octahedral sheet of the layer with the oxygen atoms of the tetrahedral sheet of one layer below. The general formula of kaolinite is $Al_2(OH)_4Si_2O_5$ and the dimensions of the unit cell are [2]: $a = 0.516\,\text{nm}$, $b = 0.894\,\text{nm}$, $c = 0.740\,\text{nm}$, $\alpha = 91.7^\circ$, $\beta = 104.9^\circ$, and $\gamma = 89.8^\circ$. The unit cell contains two formula units $[A1_2(OH)_4Si_2O_5]$.

The 2:1 clay minerals consist of two tetrahedral sheets linked to one central octahedral sheet (Figure 8.1(b)). The variety of minerals of this group (Table 8.1) arises from different types of isomorphous substitutions and cation vacancies in the octahedral sheets. The layers are uncharged (talc, pyrophyllite) or negatively charged (mica-type minerals). The charge density is mainly determined by the Al-for-Si substitutions in the tetrahedral sheets and the amount of divalent and trivalent cations within the octahedral sheets. The origin of the charges is expressed by the chemical formula

$$\underset{\text{interlayer space}}{M^{m+}_{(x+y)/m}(H_2O)_n}\underset{\text{octahedral sheet}}{[(Me^{II},\ Me^{III})^{(6-x)+}_{2-3}(OH)_2}\underset{\text{tetrahedral sheet}}{(Si_{4-y}Al_y)O_{10}]^{(x+y)}}$$

Clay minerals with about three divalent cations in the octahedral sheet per formula unit are called trioctahedral, and those with two trivalent cations are called dioctahedral. When the layers carry negative charges, cations are bound in the interlayer space for charge compensation. Generally, the interlayer space also contains water molecules, the amount of which depends on the layer charge and on the water vapor pressure around the clay particles or, in aqueous solution, on the type and concentration of salts (see Chapter 3).
The unit cell data are [2,14]:

Micas:	Biotite	$a = 0.533\,\text{nm}$; $b \approx 0.923\,\text{nm}$ $\beta = 95^\circ$	$c = 2.01\,\text{nm}$
	Muscovite	$a = 0.519\,\text{nm}$; $b \approx 0.900\,\text{nm}$ $\beta = 96^\circ$	$c = 2.00\,\text{nm}$

Vermiculites:		$a = 0.534\,\text{nm};\ b \approx 0.925\,\text{nm}$
Smectites:	Montmorillonite:	$a = 0.518\,\text{nm};\ b \approx 0.900\,\text{nm}$
	Beidellite	$a = 0.518\,\text{nm};\ b \approx 0.900\,\text{nm}$
	Hectorite	$a = 0.525\,\text{nm};\ b \approx 0.918\,\text{nm}$

Table 8.1 Classification of clay minerals [15]

Layer type	Interlayer material	Group	Species[a]	Layer charge[b]
1:1	None or H_2O only	Serpentine–Kaolin	Kaolinite, Halloysite (di)	0
2:1	None, $(x + y) \sim O$[b]	Talc–Pyrophyllite	Talc (tri), Pyrophyllite (di)	0
	Hydrated exchangeable cations, $(x + y) \sim 0.2$–0.6	Smectite	Hectorite (tri)	0.2–0.25
			Montmorillonite (di)	0.25–0.4
			Saponite (tri)	
			Beidellite (di)	0.4–0.6
			Nontronite (di)	
	Hydrated exchangeable cations, $(x + y) \sim 0.6$–0.9	Vermiculite	Vermiculite	0.6–0.9
	Nonhydrated monovalent cations $(x + y) \sim 0.6$–1	Jllite Mica	Illite	0.8–1
			Biotite, Muscovite	1

[a] Only a few examples are given. Di, tri = di- or trioctahedral structure.
[b] Layer charge in charges/formula unit.

The unit cell contains two formula units $(Si, Al)_4O_{10}$. The c spacing of the vermiculites and the smectites is not listed because it depends on the interlayer cation and the relative humidity or the solvating liquid.

The interlayer cation in smectites is mainly calcium but a few bentonites (e.g., from Wyoming) contain sodium as the interlayer cation besides calcium ions. Bentonites known as sodium bentonites do not contain pure sodium montmorillonite but sodium calcium montmorillonite with sodium and calcium in varying ratios.

Mixed-layer minerals consist of two (or more) different types of layers within the same crystals (*layer* in connection with mixed-layer minerals comprises the silicate layer itself and the interlayer space). Very important for geological studies are illite–smectite (I/S) mixed-layer minerals [16]. Common clays often contain appreciable amounts of I/S materials. Their presence in ceramic masses improves plasticity and dry strength [2]. For x-ray powder diffraction of mixed-layer minerals see Refs. [17,18].

C. Quality of Clay Mineral "Crystals"

The structure of clay minerals is characterized by different types and degrees of disorder [14,18,19]. The crystals, in particular of smectites, are never crystals in the strong sense. Many crystallographers are dismayed at the particles which clay scientists call *crystals*. In fact, a smectite *crystal* is more equivalent to an assemblage of silicate layers than to a true crystal (Figure 8.2). The particles seen in the electron microscope never have the regular shape of real crystals but look

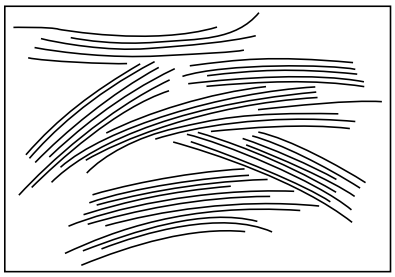

Figure 8.2 A schematic view of montmorillonite *crystals*. (From G. Lagaly and R. Malberg, *Colloids Surf.*, 49, 11–27, 1990. With permission.)

like paper torn into irregular pieces. Very instructive pictures of smectite particles were published by Vali and Köster [20]. The core of the particles is surrounded by disordered and bent silicate layers with frayed edges. Layers or thin lamellae of a few layers protrude out of the packets and enclose wedge-shape pores. The particles reveal many points of weak contacts between the stacks of the layers. At these *breaking points* the particles may easily break as under the influence of mechanical forces or during intracrystalline reaction.

In Ca^{2+} smectite crystals only a few layers form coherent domains in which all silicate layers have the same distance, for instance, corresponding to two layers of water. These domains are separated by zones composed of silicate layers in different distances because of the presence of one, three, four, or even more water layers. This structure could be clearly observed by transmission electron microscopy (TEM) inspection [21]. A few of the units composed of the coherent domains and the zones of differently spaced silicate layers are aggregated with almost parallel orientation to quasicrystals. The quasicrystals are arranged in a network with pores of different sizes, thus constituting the whole particle. The aggregated particles exhibit a very complex pore structure with lenticular pores between parallel oriented layers, pores within the network of quasicrystals and between the particles (see, electron micrographs in Ref. [22]). It seems to be possible to estimate the volumes of the different types of pores from the kinetics of water inhibition [22]. Nomenclature to name the different levels of organization is still lacking.

The structure of the smectite crystals is described here in detail because it greatly determines the type of units formed by dispersing smectites and determines the colloidal and rheological properties of the dispersions. It also governs the applicability of a bentonite in the practical uses.

The electrostatic attractions between the layers and the interlayer cations increase the stacking order in more highly charged 2:1 clay minerals. The domains with equally spaced layers become thicker and the influence of the defects on the shape and position of the (00l) reflections decreases. Defects of unequally spaced silicate layers due to different degrees of

hydration (probably a consequence of charge inhomogeneity) are still observable by delicate analysis of the x-ray reflection profiles of sodium beidellite with water monolayers [24]. The different types of layer stacking in the vermiculites were reviewed by Suquet and Pézérat [25]. Micas can be considered as true crystals, and many polymorphs were described [14]. Kaolinites also contain varying degrees of disorder in the layer stacking [14,26].

D. Layer Charge of 2:1 Clay Minerals

The 2:1 clay minerals are classified by the layer charge $(x+y)$ (Table 8.1). The most important minerals are the montmorillonites. The layer charge $(x+y)$ is given in charges/formula unit (eq/$(Si,Al)_4O_{10}$) and is, for montmorillonites, in the range $0.2-0.4$. The numerical value is identical to the interlayer cation density ξ (in equivalents of cations/mol formula unit).

The surface charge density is $(x+y)/2$ and may also be expressed as surface charge density σ_0 (in $C\,m^{-2}$). The unit cell contains two formula units $(Si, Al)_4O_{10}$ and has the dimensions a and b in the plane of the layer. The charge density is

$$\sigma_0 = 1.602 \times 10^{-19}(x+y)/ab \ (C\ m^{-2})$$

Typical surface charge densities are listed in Table 8.2.

An outstanding property of smectites and vermiculites (probably also of micas) is the nonuniform charge distribution. The density of the charges is not constant in all layers but varies from layer to layer within certain limits, and probably also from the core of the particles to the edge regions. Beidellites and vermiculites with considerably isomorphous substitution in the tetrahedral sheets can contain polar layers, i.e., both faces of a layer show different surface charge densities [27,28].

Due to the charge inhomogeneity the interlayer cation density ξ_i varies from interlayer space to interlayer space. The numerical value of ξ_i in the interlayer space i is the average of the surface charges of both layers enclosing this interlayer space. The interlayer cation density varies more or less randomly between certain limits ξ_i and ξ_j. The mean value of the

Table 8.2 Layer charge $(x + y)$, surface charge density σ_0, and equivalent area A_c of mica-type clay minerals[a]

Mineral	M[b]	$(x+y)$ (charges/formula unit)	σ_0 (C/m^2)	ab (nm^2)	A_c (nm^2/charge)
Biotite	455	1	0.326	0.492	0.246
Muscovite	390	1	0.343	0.467	0.234
Vermiculites	390	0.8	0.259	0.495	0.309
		0.6	0.194	0.495	0.412
Beidellite	360	0.5	0.172	0.466	0.466
Montmorillonites	362	0.4	0.137	0.466	0.583
		0.3	0.103	0.466	0.777
		0.2	0.069	0.466	1.165
Hectorite	380	0.23	0.076	0.482	1.048

[a] The equivalent area is the area per monovalent interlayer cation: $A_c = ab/2(x+y)$.
[b] Mean molecular mass of the formula unit $(Si_4O_{10}(OH)_2)$ without interlayer cations and water [2].

cation density $\bar{\xi}$ is equal to the mean value of the layer charge $(x+y)$. The frequency distribution of the interlayer cation densities $\xi_1, \xi_2, \ldots, \xi_j$ sometimes shows a maximum but often resembles to a bimodal distribution (cf. Figure 8.17) [27].

E. Determination of Layer Charge

The layer charge may be calculated from the chemical analysis and the cation exchange capacity. This method requires that the clay minerals be separated quantitatively from all other ancillary materials or that type, composition, and amount of these materials including the amorphous substances are exactly known. Pure microsized vermiculites are available but pure montmorillonites are never found. The amounts of accompanying minerals and amorphous silica in bentonites can be determined but the procedure is very time consuming [29]. Sometimes the content of montmorillonite in bentonites is estimated by (often somewhat suspect) methods, and the layer charge is calculated from the experimental cation exchange capacity. However, exchangeable cations are also located at the edges (see next section). If the amount of

these counterions is not considered, a too high value of the layer charge is obtained.

The most reliable method for determining the layer charge is exchanging the interlayer cations by a series of primary n-alkylammonium ions $C_nH_{2n+1}NH_3^+$. These ions are quantitatively exchanged for the interlayer cations (and the cations at the external surfaces). The arrangement of these ions in the interlayer space depends on the chain length n and the charge density in the interlayer space. The different types of interlamellar arrangements are recognized by the basal spacing which is measured by simple x-ray powder technique. The exact layer charge is derived from the basal spacing measurements [27,30–32]. Primarily, the interlayer cation density $\bar{\xi}$ is obtained, which is numerically identical to the layer charge $(x+y)$, both in eq/mol. With an average molecular mass of the formula unit of smectites (without interlayer cations and water) of ~360 the exchange capacity related to the interlayer cations is

$$C_i = \xi/360 \quad \text{(eq/g silicate)}$$

For smectites, the interlayer exchange capacity is about 80% of the total exchange capacity C_t. (For determinative methods for the total cation exchange capacity, see Ref. [33].)

The decisive progress brought about by the alkylammonium method is the evaluation of the charge heterogeneity. When the charge density changes from interlayer space to interlayer space, the arrangement of the alkylammonium ions in the interlayer spaces varies accordingly and, in characteristic ways, influences the position and shape of the (00l) reflections in the x-ray powder pattern. By a simple procedure [30] the charge heterogeneity is deduced from the x-ray powder patterns, and diagrams (as in Figure 8.17) are constructed which reveal the frequency distribution of the interlayer cation densities ξ_i. The mean interlayer cation density $\bar{\xi}$ is obtained from

$$\bar{\xi} = \frac{\sum \nu_i(\xi_i + \xi_{i+1})/2}{\sum \nu_i},$$

where ν_i is the frequency of interlayer spaces with a density between ξ_i and ξ_{i+1}. The mean cation density $\bar{\xi}$ is equal to the mean layer charge $(x+y)$.

F. Edge Charges

The sign and density of the charges at the crystal edges depend on the pH of the dispersion. Sometimes clay scientists still use the term *broken bonds*, which a colloid scientist never will use. The charging arises from adsorption or dissociation of protons as in case of oxides (Figure 8.3). In acidic medium, an excess of protons creates positive edge charges, and its density decreases with rising pH. Negative charges are produced by the dissociation of silanol and aluminol groups [34].

The interesting question concerns the condition that leads to virtually uncharged edges. When alkylammonium ions were exchanged at pH = 6.5, the total amount of alkylammonium ions bound by Wyoming montmorillonite was 1.07 meq/g silicate (average value, see Table 8.3). The interlayer cation exchange capacity was 78 meq/g silicate. Thus 0.29 meq alkylammonium ions were bound at the edges (or 27% of the

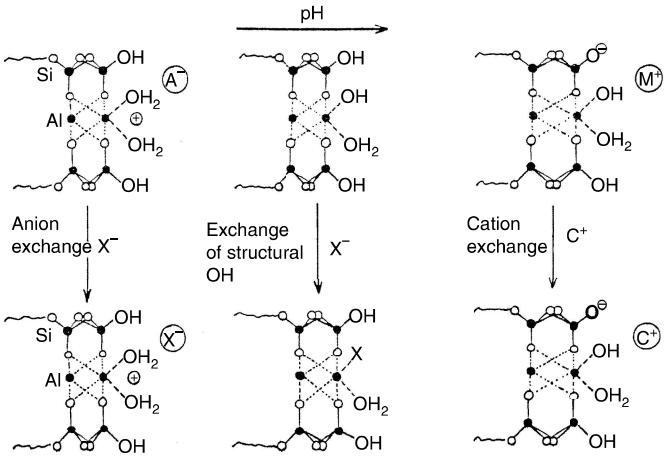

Figure 8.3 The pH-dependent ion and ligand exchange reactions at the edges of the clay minerals crystals. (From K. Jasmund and G. Lagaly, Tonminerale und Tone, Figure 3.1. Ref. 2. With permission.)

Table 8.3 Total (C_t) and interlayer exchange capacity (C_i) of Montmorillonite[a]. C_t from the carbon content of the alkylammonium derivatives, C_i by the alkylammonium method

n[b]	C_t (meq/g silicate)	C_i/C_t
6	1.06	0.74
8	1.06	0.74
10	1.10	0.71
12	1.07	0.73
14	1.01	0.77
16	1.10	0.71
18	1.12	0.70

[a] From Wyoming, type "Greenbond" M 40, supplied by Süd-Chemie AG in 1974.
[b] Number of carbon atoms of the alkylammonium ions.

total exchange capacity). A very similar result was obtained by surface charge measurements with the particle charge detector. This simple instrument indicates the point, at which all charges of a colloidal particle are compensated by macroions or, in our case, by the alkylammonium ions. The amount of alkylammonium ions required to uncharge the particles increased rapidly with pH because in acidic medium protons strongly competed with the alkylammonium ions also in the interlayer space. At pH = 6–8, a plateau was reached and, in agreement with the analytical data, a dosage of 1.03 meq alkylammonium ions/g montmorillonite uncharged the particles. The increase at higher pH was caused by the presence of alkylamine molecules, which were strongly adsorbed by alkylammonium montmorillonite.

The total amount of alkylammonium ions bound by 2:1 clay minerals is often slightly higher than the total cation exchange capacity determined by other methods [2,33]. This is a consequence of the charge regulation at the edges. Adsorption of surface-active agents on oxidic surfaces increases the surface charge density by adsorption (anionic surfactants) or desorption (cationic surfactants) of protons [35,36]. Thus, adsorption of alkylammonium ions exceeding the cation

exchange capacity is accompanied by desorption of protons from surface OH groups. The analytical data clearly reveal that, at pH 6.5, a considerable amount of cations are bound at the edges. The point of zero charge of the edges must be below 6.5, probably around pH = 5.

The flow behavior of sodium montmorillonite dispersions in water or diluted NaCl solutions shows characteristic changes with pH (Section VII.A). The shear stress decreases strongly above pH = 4.5 (Figure 8.25). This reduction of viscosity is generally attributed to the destruction of the card-house when the amount of positive edge charges becomes too small to stabilize the card houses by stable edge(+)–face(−) contacts [37,38]. Thus, rheological measurements also indicate an apparent p.z.c. of the edges at pH = 5 or slightly above.

The point of zero charge at the edges of colloidal pyrophyllite particles ($x+y \sim 0$, Table 8.1) was found at pH = 4.2 by titrations at various indifferent electrolyte concentrations [39].

G. Intracrystalline Reactions

Exchange of interlayer cations by other inorganic and organic ions is one of the outstanding properties of 2:1 clay minerals. A diversity of other reactions has to be mentioned including reversible hydration and solvation, displacement of interlamellar water by organic molecules, interlamellar complexation, and sorption of organic derivatives in the interlayer spaces (Figure 8.4). Electron transfer from or to the layers is the basis of several catalytic reactions [2,40–43].

Kaolinite intercalates several organic compounds [41]. Hydrated kaolinites are prepared by displacement of suitable organic guest molecules (e.g., dimethylsulfoxide) by water [44]. A variety of organic molecules can be intercalated in these hydrated kaolinites to give ordered or less ordered intercalates [45]. A refined displacement method consists of reacting kaolinite with NMF (giving a basal spacing of 1.08 nm), which is replaced by methanol (basal spacing 1.11 nm). The wet kaolinite–methanol intercalation compound is then treated with the methanolic solution of the final guest compound [46].

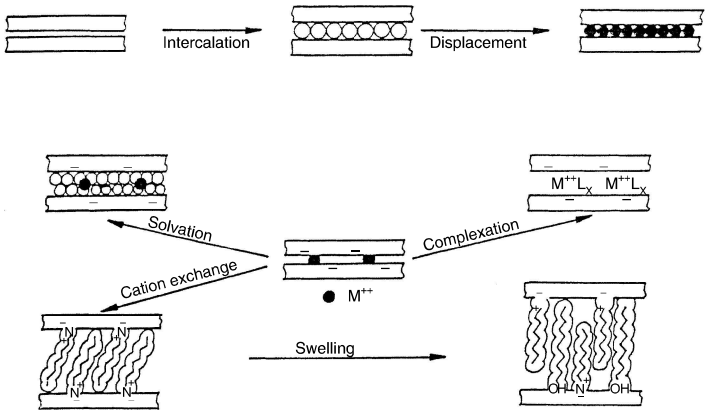

Figure 8.4 Intracrystalline reactions of 1:1 and 2:1 clay minerals.

III. THE CLAY–WATER SYSTEM

A. Hydrates of 2:1 Clay Minerals

The 2:1 clay minerals form hydrates with one, two, three, or four layers of water between the silicate layers. The state of hydration varies with the water vapor pressure, the water content, and, in salt solutions, with the type and concentration of salts, and is dependent on the layer charge and the interlayer cation density. Typical basal spacings are: 1.18–1.24 nm (water monolayers), 1.45–1.55 nm (water bilayers), and 1.9–2.0 nm (four water layers).

The changes of the basal spacing with the salt concentration are seen in Figure 8.5. The dotted fields comprise the spacings of a large collection of smectites and vermiculites. Sodium smectites change from a state indicated by a basal spacing $\rightarrow \infty$ (see Section III.C) into hydrates with four, and, at higher salt concentration, two layers of water [47]; vermiculites persist in the two-layer hydrate over the whole range of concentrations. Potassium ions in higher concentrations restrict the interlayer expansion of the smectites to water monolayers. The hydration of vermiculites is virtually impeded by KCl solutions at concentrations above 0.01 *M*. In

the presence of calcium ions the four-layer hydrate of smectites and the two-layer hydrate of vermiculites persist over a wide range of concentrations.

The variation of the basal spacings with salt concentration (Figure 8.5) is of great interest to colloid scientists. To explain the reversibility of salt coagulation of many colloidal dispersions, Frens and Overbeek [48,49] introduced the concept of the distance of closest approach. They postulated that at the onset of coagulation the particles are not in direct contact but remain separated by a certain distance. A value of 0.4 nm (corresponding to two water layers) was shown by a number of calculations as the most probable minimum separation. That a distance of closest approach really exists is clearly seen by the behavior of sodium and calcium smectites as well as sodium and calcium vermiculites in NaCl and $CaCl_2$ solutions. Even far above the critical coagulation concentrations and up to concentrations as high as $5\,M$ NaCl the silicate layers remain separated by two water layers. The water layers are displaced from between the surfaces only when the counterions like potassium ions are attracted to the surface by specific interactions. The *fixation* of potassium ions (and cesium and rubidium ions) is well known to clay scientists and is explained by the reduced hydration energy and a better geometric fit of the potassium ions into the surface oxygen hexagons in comparison to sodium ions (cf. Ref. [50]).

B. Structure of the Hydrates

The hydrated forms of 2:1 clay minerals may be considered as quasicrystalline structures because there is a certain amount of order in the interlayer space. The counterions (interlayer cations) reside near the middle plane of the interlayer spaces [51–53]. The silicate layers of the more highly charged silicates (saponites, vermiculites) assume ordered or semiordered layer-stacking sequences [25]. In smectites, the superposition of the layers is generally random (turbostratic structure) but specimens with a certain periodic structure (e.g., beidellites) are also found [54,55]. The layers of Wyoming montmorillonite

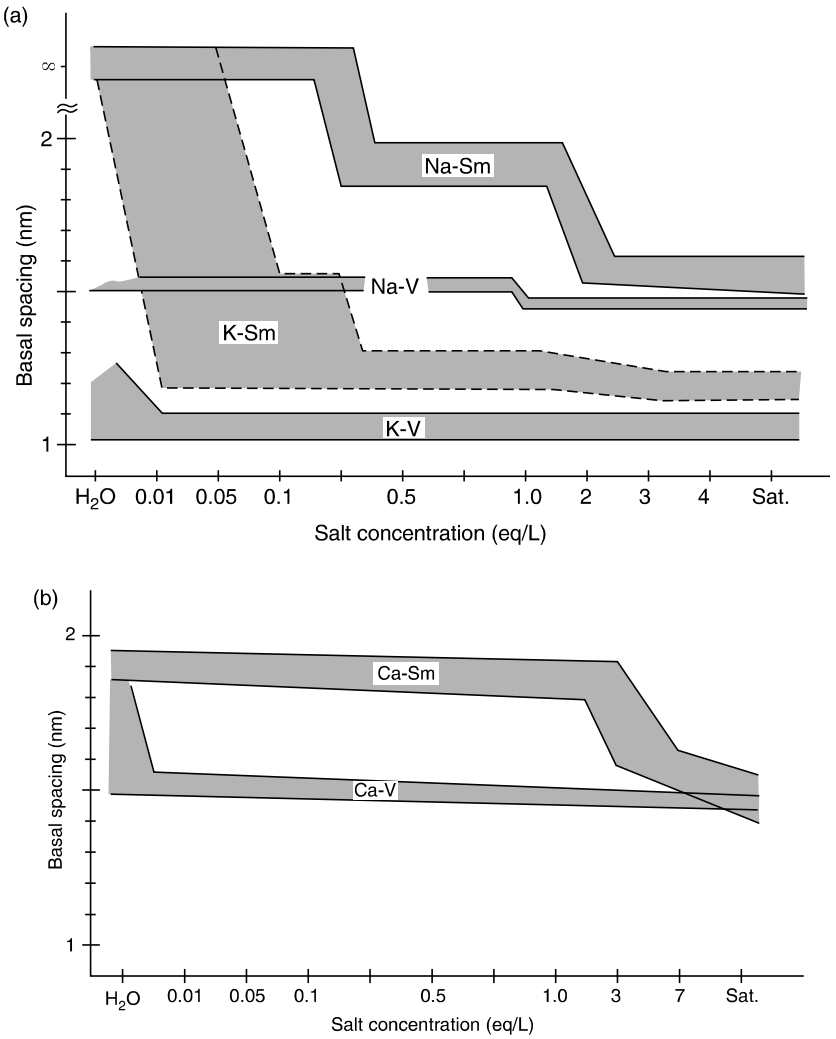

Figure 8.5 Basal spacing of 2:1 clay minerals as a function of salt concentration. Na–Sm, sodium smectites and NaCl; K–Sm, potassium smectites and KCl; Ca–Sm, calcium smectites and $CaCl_2$; Na–V, sodium vermiculites and NaCl; K–V, potassium vermiculites and KCl; and Ca–V, calcium vermiculites and $CaCl_2$. (From G. Lagaly and R. Fahn, in *Ullmann's Encyclopedia of Technical Chemistry*, 4th ed., Vol. 23, Verlag Chemie, Weinhein, 1983, pp. 311–326. With permission.)

with initially random superposition become more and more regularly stacked after wetting and drying cycles in the presence of potassium ions [56].

Organization, mobility, and dynamics of the interlayer water molecules were studied in great detail by Fripiat (see, for instance, Refs. [53,57–60]). Generally, a part of the water molecules form the hydration shells around the interlayer cations, the other water molecules fill the space between the hydration shells [61] and are in a state probably similar to the state around structure-breaking ions. There is no doubt that the properties of interlayer water are different from those of bulk water [62], e.g., showing increased acidity [53,59–65] and rotational correlation times about two orders of magnitude ($\sim 10^{-10}$ s) lower than in liquid water [59].

Grandjean and Laszlo [66] deduced from deuterium nuclear magnetic resonance (NMR) studies of montmorillonite–water dispersions (0.024 g/ml D_2O) that the water molecules are strongly polarized and are simultaneously bound to a negative center by a hydrogen bridge and to an interlayer cation by electrostatic forces. As a consequence, the acidity of interlayer water molecules is increased. In sodium montmorillonite the water molecules reorient predominantly around the hydrogen bond whereas they reorient around the metal–oxygen axis in the presence of calcium ions.

A question of importance concerns the influence of the surface force fields of the external surfaces onto the water structure around and between the particles. Fripiat et al. [59,60] could not detect long-range forces acting on the water molecules outside of the particles, neither at the thermodynamic scale (heat of immersion measurements) nor at the microdynamic range (NMR measurements). The number of water layers influenced by the surface forces is 3–4, i.e., a water film of thickness of about 1 nm. In contrast, Mulla and Low [67] concluded that the molecular dynamics of vicinal water as seen by infrared spectroscopy is affected by the particle surface to an appreciable distance of about 4 nm.

Molecular dynamics simulations of the montmorillonite hydrates mainly confirm the experimental results on the position of the interlayer cations and the interlayer water

structure. A part of the lithium interlayer cations form inner-sphere surface complexes (the lithium ions are directly coordinated to the surface oxygen atoms). The expansion of the interlayer space is accompanied by the conversion in outer-sphere surface complexes to diffuse layer species as a result of the strong Li^+–water interactions. However, a part of Li^+ ions still persist as inner-sphere surface complexes but are in ready exchange with the diffuse layer Li^+ [68]. Also, sodium and potassium ions have a significant coordination with surface oxygen atoms and exist in inner- and outer-sphere surface complexes [62,69–71]. Increasing tetrahedral substitution shows a trend of direct binding between Na^+ and surface oxygen atoms and a corresponding dissimilarity with the coordination structure in bulk solution. The coordination structure of water molecules around K^+ ions is, as expected, not nearly so well defined as it is for Li^+ and Na^+ ions. Magnesium counterions on montmorillonite reside at the midplane of the interlayer spaces. Nonsolvating water molecules move freely on planes above and below the midplane. In the case of beidellites, the motion of water molecules is more hindered because of the presence of negative charge sites close to the surface [72]. Surface energy studies by contact angle measurements also indicated that divalent cations are shielded from the silicate surface by water molecules whereas monovalent cations can be in direct contact with the surface oxygen atoms [73].

C. Structure with Diffuse Ionic Layers

In Figure 8.5 the basal spacing $\rightarrow \infty$ is indicated for sodium (and several potassium) smectites in water or diluted salt solutions ($< 0.2\,M$ for NaCl). This is an outstanding property of smectites with monovalent counterions. The crystals delaminate into the individual silicate layers, or thin packets of them, and form a colloidal dispersion of very thin particles (Figure 8.6). The thickness and width of the individual layers and lamellae produced by the disarticulation of a large variety of smectites and illite–smectite mixed-layer crystals (see Section IV.D) were recorded by TEM [74,75]. The interlayer cations constitute the diffuse ionic layers around

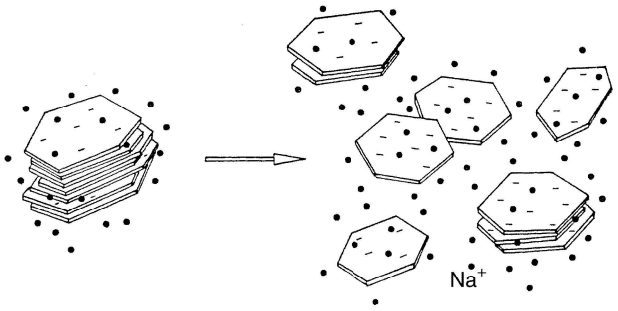

Figure 8.6 Disarticulation (delamination) of alkali smectite crystals in aqueous dispersions.

the silicate layers and silicate lamellae. The presence of discrete particles that do not interact strongly and flow independently was proven by light and small-angle neutron scattering (SANS) [9,76].

The average interparticle distances (obtained from small-angle scattering) respond to the addition of sodium salts in an almost linear decrease with $2/\sqrt{c}$ (c = salt concentration) until, at $c \approx 0.2$ mol/l, rearrangement into the quasicrystalline structure is seen by the sudden decrease of the spacing from about 4 to 2 nm [3,77].

With counterions other than lithium and sodium the distances between the individual layers are no longer equal (or, more correctly, varying around a mean value). Tactoids are formed by a columnar-like superposition of a few silicate layers in equal distances. The distances between the tactoids are larger than within these units. In Figure 8.7 the relative number N/N_{Li} of plates per tactoid ($N_{Li} = 1$ for lithium as counterion) when the calcium ions are progressively replaced by alkali and magnesium ions [76] is shown. In the presence of calcium ions the tactoids contain about seven silicate layers. Even small amounts (< 0.2 equivalent fractions) of alkali metal ions reduce the size of the tactoids dramatically to one to three layers.

Cebula et al. [78] concluded from small-angle neutron-scattering measurements that a considerable part of the

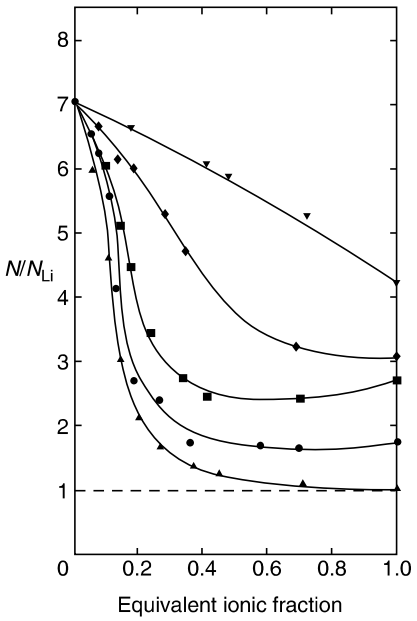

Figure 8.7 Relative number of layers per tactoid, N/N_{Li} ($N_{Li} = 1$) as a function of surface coverage when the calcium ions are exchanged by lithium (▲), sodium (●), potassium (■), cesium (◆), and magnesium (▼) ions. (From L.L. Schramm and J.C.T. Kwak, *Clays Clay Miner.*, 30, 40–48, 1982. With permission.)

layers is aggregated to units consisting of two silicate layers (potassium montmorillonite) or three silicate layers (cesium-montmorillonite) interleaved with bimolecular water layers.

D. Effect of Calcium Ions

The interaction between the dispersed clay mineral particles or silicate layers is described by the DLVO theory [79–81] even if reasons were put forward that other types of interactions must be considered [82–84]. One effect is difficult to explain by the DLVO theory. It is the pronounced sensitivity of the colloidal clay mineral dispersions against calcium ions (and other di- and trivalent metal ions). In the presence of

these ions, the particles remain in coagulated state and cannot be dispersed even in pure water.

Fitzsimmons et al. [85] showed that, just after contact of sodium montmorillonite dispersions with calcium-saturated exchange resins, calcium montmorillonite existed as single platelets as in the sodium form. With time the individual silicate layers aggregated by overlapping of the edges and linked together to form flat, large sheets (band-like aggregation; see Section VII.A).

As revealed by the basal spacings (Figure 8.5), calcium ions maintain the quasicrystalline structure. They reside in the middle of the interlayer space, restrict the interlayer distance to 1 nm (basal spacing 2 nm), and impede transition into the structure with diffuse ionic layers. The effect of calcium ions is, therefore, related to the question of whether the quasicrystalline structure with electrostatic attraction between the layers can rearrange into the state with ionic double layers.

A first attempt to explain the attractive interactions in the presence of calcium ions was developed on the basis of the DLVO theory by Kleijn and Oster [86]. The counterions located between the layers are assumed to be in equilibrium with the bulk solution, so that their charge density was slightly different in magnitude from the charge density of the layers. The electrostatic contribution to the Gibbs energy, G_e, was calculated for constant surface charge density (see also Ref. [79]). The Gibbs energy was positive over a wide range of salt concentrations c_s and surface charge densities σ_0 when the counterions were monovalent. For smectites with $\sigma_0 = 0.07$–0.14 C/m^2 (Table 8.2) the electrostatic interaction was repulsive at $c_s < 10^{-1}\,M$. Thus, sodium montmorillonite particles were coagulated by salt concentrations slightly above $0.1\,M$ as long as the surface charge density remained below 0.1 C/m^2 and by salt concentrations slightly below $0.1\,M$ for $\sigma_0 = 0.1$–0.15 C/m^2. For more highly charged clay minerals (vermiculites, micas) the Gibbs energy was negative even at very low salt concentrations, and the formation of colloidal dispersions was not expected. With divalent counterions the colloidal dispersions not only of more highly charged clay

minerals but also of very low-charged smectites became unstable at $c_s < 10^{-3}$ M, and colloidal dispersions were not formed.

More recently, Kjellander et al. [87] calculated the diffuse double-layer interactions with an advanced statistical mechanical method. In contrast to the predictions of the simple Poisson–Boltzmann theory this model gives strongly attractive double-layer interactions for divalent ions (Figure 8.8). The position of the potential minimum is in reasonable agreement with the x-ray basal spacing measurements. The most important reason for the occurrence of the potential minimum is the attraction due to the ion–ion correlation. In the Gouy–Chapman model of the diffuse ionic layer the correlation between the ions is entirely neglected, i.e., the ion density in the neighborhood of each ion is assumed to be unaffected by this ion. This neglect of the ion–ion correlation is a reasonable approximation when the electrolyte concentration *and* the surface charge density are sufficiently low. If any of these conditions are violated, the correlation between the ions must be considered and can lead to attractive double-layer interactions between equally charged particles at short separations [88]. This correlation influences the interaction by two different mechanisms: they make the ion concentration in the middle of the interlayer space change and they contribute to an attractive electrostatic fluctuation force [88].

IV. HOW COLLOIDAL CLAY MINERAL DISPERSIONS ARE PREPARED

A. Purification of Clays

In most cases, natural products are used in studying the properties of clay mineral dispersions. Clay minerals having a certain degree of purity are separated from the clays by sedimentation techniques. The first step consists of removal of iron oxides and organic materials. These materials not only affect properties of the colloidal dispersions but also prevent optimal peptizing of the clay particles and successful fractionation by sedimentation. Iron oxides are removed by reduction

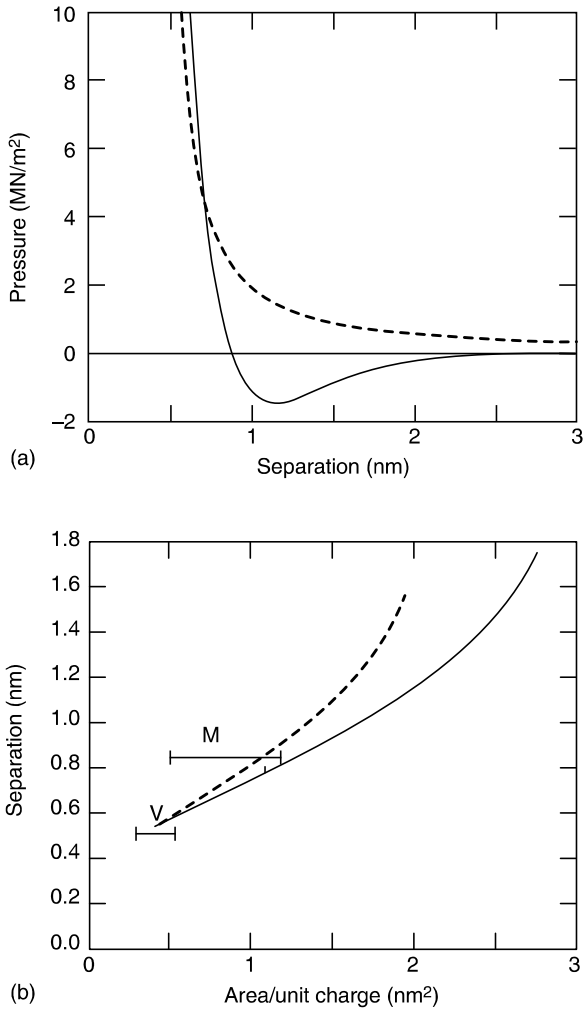

Figure 8.8 Calculation of the pressure between two silicate layers of calcium montmorillonite and vermiculite. (a) Total pressure, calculated for montmorillonite with a surface charge density $\sigma_0 = 0.12$ C/m^2 (full line); results of the DLVO theory shown as dotted line. (b) Position of the potential minimum as a function of the area per unit charge. Solid line: the total net pressure; dotted line: pressure without van der Waals interaction included. (M), montmorillonites; (V), vermiculites. (From R. Kjellander, S. Marčelja, and J.P. Quirk, *J. Colloid Interf. Sci.*, 126, 194–211, 1988. With permission.)

with sodium dithionate in the presence of citrate ions as complexing agents for the Fe^{2+} ions. Organic materials are decomposed to CO_2 by oxidation with H_2O_2. (For experimental details, see Refs. [89–92].)

There is a certain risk that during decomposition of the organic materials low molecular weight substances form which are adsorbed by the clay minerals. Significant amounts of oxalate were found when clays with high contents of organic matter were oxidized with H_2O_2. Most of it was present as soluble oxalato aluminate but a part was attached to the clay mineral [93]. Oxalate adsorption on sodium smectites showed a complex behavior. At low initial oxalate concentrations the amount adsorbed (in the range of 0.1–1 mg/g) decreased with pH. When the initial concentration of oxalate exceeded 0.003 mol/l, the amount adsorbed showed a sharp minimum at pH = 6–7 [94]. Other oxidizing agents, which may be used to decompose the organic materials, are sodium hypochlorite [95] and bromine water [96].

Sometimes the organic material is difficult to remove quantitatively, e.g., when polymeric materials have penetrated into the interlayer spaces and are protected from thermal and chemical degradation.

Other materials that generally have to be removed are calcium and magnesium carbonates and amorphous silica. Carbonate is decomposed by acids, and silica is dissolved by boiling in Na_2CO_3 solution [92]. The carbonates deliberate calcium or magnesium ions, which reduce the degree of peptization. Amorphous silica can act as cementing agent between the particles.

B. Fractionation of Clays

Particle size fractionation of clay is necessary to separate the clay minerals as well as possible from ancillary materials. A decisive step in preparing a stable dispersion of the clay is the replacement of divalent counterions by sodium (or lithium) ions. Large amounts of sodium ions are introduced during the removal of iron oxides and humic materials. Nevertheless, it is recommended to react the clay with a sodium chloride

solution (about 1 M) several times further to remove all calcium ions (or other divalent ions). It should be noted that during and after the sodium for calcium exchange the clay cannot be intensively washed with water because the smectites begin to disperse into the colloidal state and are very difficult to filtrate or separate by centrifugation. Finally, the excess of salts must be removed. As dilution with water immediately leads to peptization of the sodium smectite, the only reliable way is to dialyze the dispersion against water. The pH of the dispersion should be maintained at 7–8 (adjusting with some drops of NaOH) because the clay particles aggregate at pH below 6.5.

The final dispersion obtained by dialysis and adjusted to pH 7.5 is stable and contains the particles in an optimal degree of dispersion. The addition of deflocculating agents like phosphates and polyphosphates is not required to attain the colloidal distribution. This is verified by Figure 8.9. The particle size (obtained by a Horiba particle size analyzer) of three fractions of two montmorillonites was independent of the amount of calgon (polyphosphate) added as peptizer. A similar plot was obtained for phosphate as the dispersing agent.

The stable dispersion of the clay minerals in homoionic form is fractionated by sedimentation in the gravitational or, for particle sizes below <2 μm, in the centrifugal field (for details, see Ref. [92]). To reduce the particle–particle interaction during sedimentation, the volume fraction of the particles should be in the range 10^{-3}–2×10^{-3} (about 5 g clay/1000 ml water). The particle size of the fractions is expressed in Stokes equivalent spherical diameters.

The colloidal dispersions obtained may be used as such or concentrated by water vapor evaporation at about 60°C, e.g., in a rotary evaporator. When these dispersions are stored for some time, they must be kept in the dark and refrigerated. Drying of the aqueous dispersions yields compact dense materials that are difficult to redisperse. Freeze-drying or washing with acetone and air-drying are recommended to obtain a fine powder. However, it is advisable to avoid the drying steps because the smectites may not be completely redispersed.

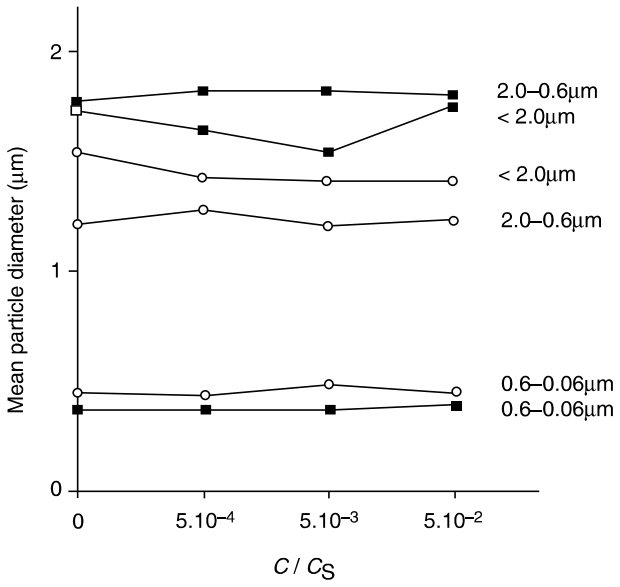

Figure 8.9 Mean particle size of different fractions of two montmorillonites versus the concentration c/c_s of polyphosphate added; c_s: concentration at saturation at room temperature. ■, montmorillonite (Wyoming); ○, montmorillonite (Niederschönbuch, Bavaria). The mean particle size of the different fractions was measured with the Horiba centrifugal particle size distribution analyzer, CAPA-500.

C. Dispersions of Kaolin

The plate widths of kaolinite particles vary from about 0.1 to 20 µm [4]. Cumulative particle size distribution curves of four kaolins are shown in Figure 8.10. Kaolinite particles are often found as largely composed of pseudohexagonal plates [97–99]. The content of ancillary minerals (feldspars, quartz, mica, and smectites) varies with particle size. Figure 8.11 shows that pure dispersions of kaolinite can be obtained from certain kaolins by selecting the appropriate particle size fractions. In fractions <0.1 µm, smectites are enriched; in fractions >1 µm, quartz, feldspars, and micas become abundant. However, the variation of the composition with particle size

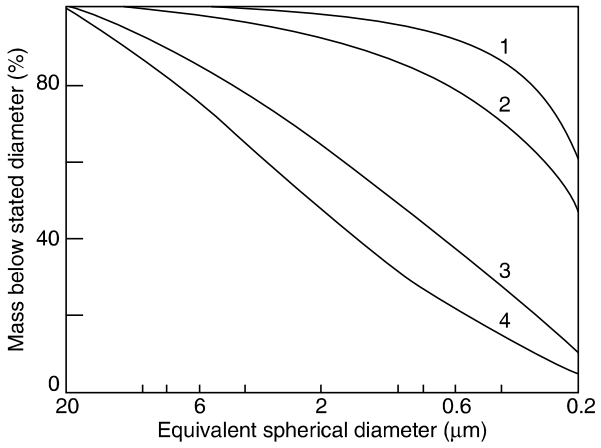

Figure 8.10 Cumulative particle size distribution curves of kaolins: curves 1 and 2, sedimentary kaolins from eastern Georgia; curve 3, sedimentary kaolin from central Georgia; curve 4, primary kaolin from Cornwall. (From I.E. Odom, *Philos. Trans. R. Soc., London A*, 311, 391–409, 1984. With permission.)

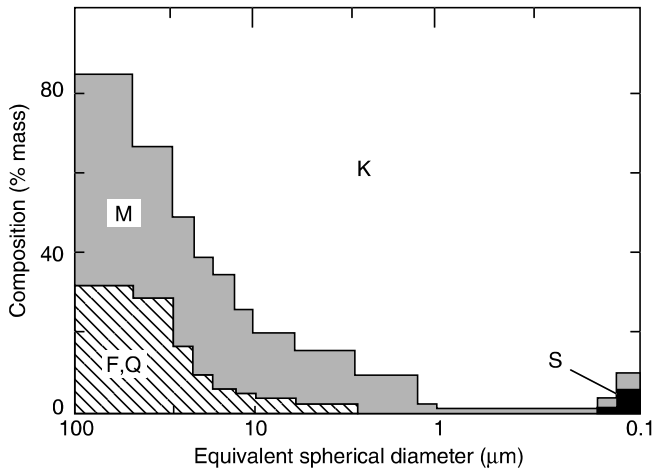

Figure 8.11 Mineral composition of Cornish kaolin with particle size. (F, Q) feldspars and quartz; (M) mica; (S) smectites; (K) kaolinite. (From W.B. Jepson, *Philos. Trans. R. Soc., London A*, 311, 411–432, 1984. With permission.)

depends on the deposit and, in many other cases, dispersions of pure kaolinite cannot be obtained by fractionation.

When the hydrogen bonds and the dipole interactions which hold together the silicate layers of kaolinite crystals are weakened by intercalation of suitable organic molecules, the crystals can be separated into thinner lamellae under the action of mechanical forces. This reaction has been used by Chinese ceramists to improve the quality of porcelain [100]. Stable colloidal dispersions of kaolinite lamellae can be prepared by partial delamination of the particles when kaolinite is treated with DMSO and ammonium fluoride [101]. Ammonium fluoride is added because exchange of some OH^- groups by F^- ions reduces the number of hydrogen bonds and the bonding energy between the layers [44].

D. Dispersions of Smectites and Vermiculites

Smectite particles may be as large as 2 μm and as small as 0.1 μm with average sizes of about 0.5 μm [3,102]. The morphology of individual particles ranges from lamellar to lath and even to fiber shapes, but mostly the particles are of irregular shape. Aggregates may be compact, foliated, or reticulated [99,103].

The singular processes proceeding during fractionation of smectites by sedimentation distinguishes smectites from all other clay minerals. Pretreatment reactions and saturation with sodium ions causes an increasing delamination: the particles disarticulate into the individual silicate layers during sedimentation. The particles, whose equivalent diameter is measured by sedimentation are artificial products and are not the same particles originally present in the bentonite. Nevertheless, fractionation is a sensitive tool for detecting differences between bentonites of different origin. A bentonite consisting of particles of various thickness and plate widths may be fractionated by sedimentation at conditions whereby all particles are delaminated. The mass content of the different particle size fractions is then representative of the number of silicate layers with a given diameter (mean spherical equivalent diameter), which originally were aggregated to

thicker crystals. Naturally, nothing can be said about the thickness of the original particles. Thus, the particle size distribution obtained by fractionation represents the plate width distribution in the parent bentonite. A bentonite, which produces fractions of very fine particles, must contain particles of small diameters. In fact, bentonites of various deposits differ mainly in the particle size distribution below 2 μm (Figure 8.12).

As many montmorillonites are formed by alteration and weathering reactions, the differently sized particles may not be identical in layer charge. However, the mean layer charge of the particles of various fractions often changes only slightly [32]. For instance, the layer charge of montmorillonite of Wyoming only increases from 0.27 charges/formula unit (<0.06-μm fraction) to 0.28 charges/formula unit (2- to 63-μm fraction). The Bavarian montmorillonite (bentonite from Niederschönbuch) shows similar changes: 0.27 charges/formula unit for <0.06-μm particles and 0.29 charges/formula unit for 2- to 63-μm particles. However, distinct changes of the charge distribution curves are observed. During peptization and fractionation, the particles are completely disarticulated. Afterward the layers are reaggregated by coagulation, and the sequence of the differently charged layers (as a consequence of charge heterogeneity, see Section V.C) must not be the same as in the parent material. Dialysis can also change the charge distribution to some extent, not only because of the disaggregation–re-aggregation mechanism but also because of the increased risk of chemical attack on the thin silicate layers [32].

As a consequence of the disarticulation of smectite *crystals* into the individual silicate layers (Figure 8.6), illite–smectite mixed-layer *crystals* can disintegrate at the low-charged interlayer spaces. The type of the produced fundamental particles (Section V.C) depends on the charge distribution, that is the variation of the cation density from interlayer space to interlayer space (Figure 8.13). The particles do break up only at the interlayer spaces with cation densities typical of smectites. The way in which the I/S mixed-layer crystals delaminate has technical consequences because

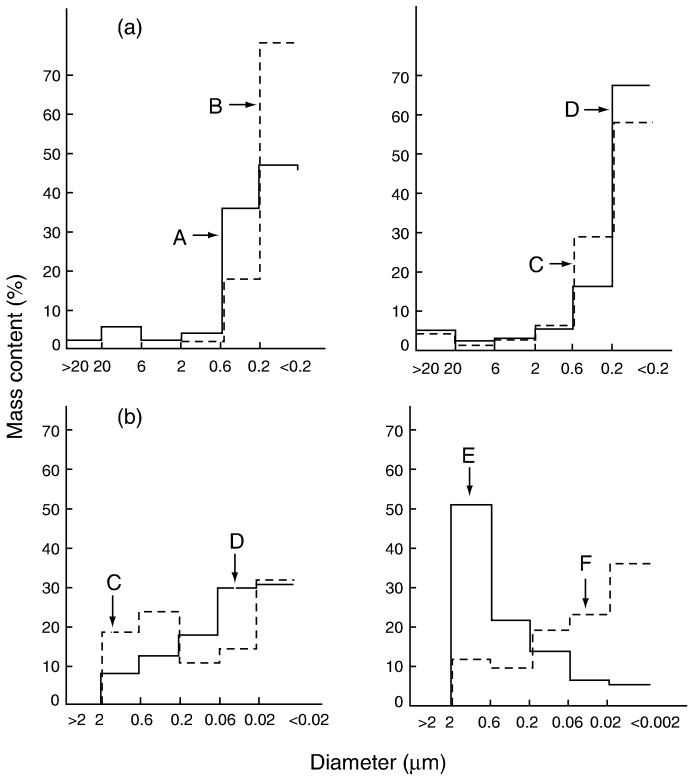

Figure 8.12 Particle size distribution of several bentonites. (a) Mass content, related to the original material; (b) Mass content, related to the fraction $<2\,\mu m$. A, bentonite, Kumhausen, Bavaria; B, *Tixoton*, Kumhausen, Bavaria; C, bentonite, Belle Fourche, Dakota; D, bentonite, Amory, Mississippi; E, bentonite Cameron, Arizona; F, bentonite, Schwaiba, Bavaria. (From G. Lagaly and R. Fahn, in *Ullmann's Encyclopedia of Technical Chemistry*, 4th ed., Vol. 23, Verlag Chemie, Weinhein, 1983, pp. 311–326. With permission.)

many common clays contain I/S materials. The different types of particles produced by the break-up of the mixed-layer crystals of soda-activated clays determine the flow behavior of these dispersed clays (see also Ref. [38]).

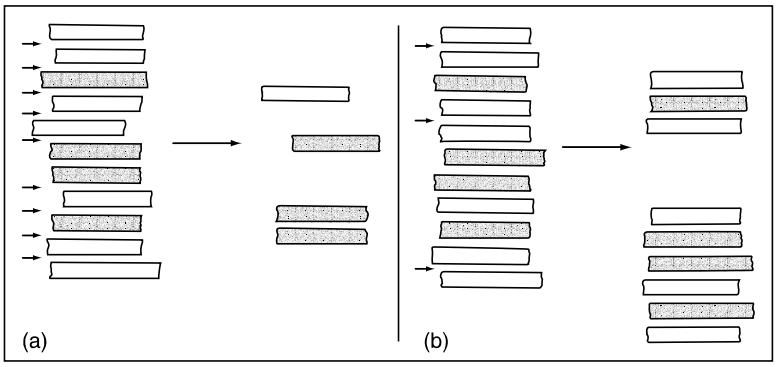

Figure 8.13 Delamination of I/S mixed-layer crystals. Different types of fundamental particles form depending on the variation of the interlayer cation density, i.e., the charge distribution. The particles are only split at the interlayer spaces with sufficiently low cation densities (arrows).

Submicron vermiculite particles could be prepared from macroscopic vermiculite flakes by ultrasound treatment [104].

E. H^+-Saturated Smectites

Sometimes it is desirable to prepare dispersions of H^+-saturated smectites. Leaching of smectites with acids results in a high degree of H^+ saturation and is accompanied by a severe chemical decomposition of the layers. The aluminum ions (also magnesium and other divalent ions) deliberated by the decomposition are preferentially adsorbed and the remaining structure progressively transforms into the Al^{3+} form [34,105]. In the initial states, the dispersion is stable for a certain time [106]. With increasing alteration, the amount of deliberated aluminum ions causes coagulation. Barshad [107] recommended passing a sodium smectite dispersion (1–2%) rapidly (200 ml/1–5 min) through a train of three exchange resin columns arranged in the order of H^+ resin $\rightarrow$ HO^- resin $\rightarrow$ H^+ resin. An H^+-saturated, highly peptized smectite dispersion is obtained which remains stable for some time.

V. COAGULATION OF CLAY MINERAL DISPERSIONS

A. Stability Against Salts

Well-dispersed clay minerals in the sodium form are coagulated by very small amounts of salts. For NaCl, the critical coagulation concentration c_K varies between 3 and 15 mmol/l:

- Kaolinites, 7–12 mmol/l [108]; 5–10 mmol/l [109]; 16–40 mmol/l (for pH increasing from 4 to 10, Figure 8.14(a) [110]).
- Montmorillonites, 7.8 mmol/l [111]; 3.5 mmol/l [112]; 8 mmol/l (pH $\approx$ 7 [113]); 1–10 mmol/l (for pH increasing from 4 to 10, Figure 8.14(b) [110]); 7–20 mmol/l (pH = 7), 17–68 mmol/l (pH = 9.5) [114]; 8–15 mmol/l (for two montmorillonites and different particle sizes at pH = 6–7 [115]); 12 mmol/l [116]; 10–44 mmol/l (for pH increasing from 5 to 9.8 [117]); 15–32 mmol/l (for pH increasing from 6.4 to 9 [118]).
- Beidellite, 5–7 mmol/l (pH = 6–7 [115]).

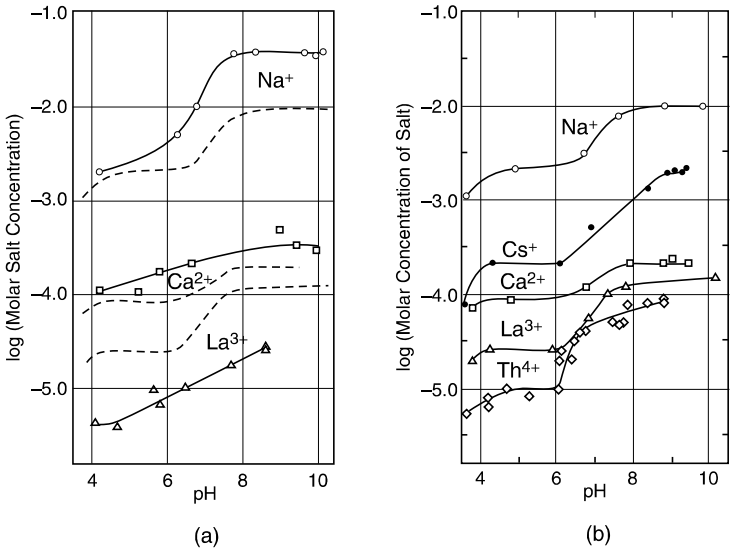

Figure 8.14 (*Continued*)

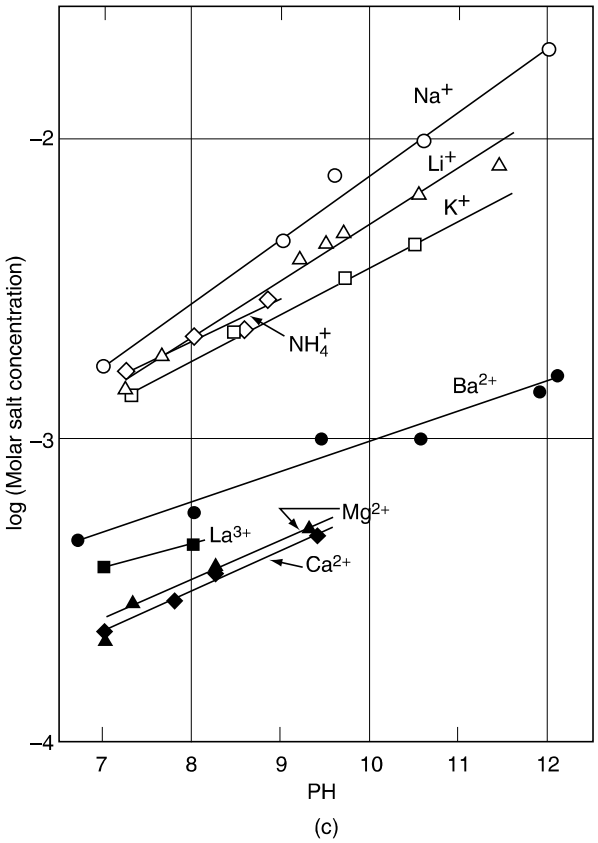

Figure 8.14 Critical coagulation concentration of various nitrates (counterions indicated) as a function of pH. (a) Dispersions of kaolinite (25 ppm); dotted line: sodium montmorillonite for comparison. (From L.S. Swartzen-Allen and E. Matijević, *J. Colloid. Interf. Sci.*, 56, 159–167, 1976. With permission.) (b) Dispersions of sodium montmorillonite (250 ppm). (From L.S. Swartzen-Allen and E. Matijević, *J. Colloid Interf. Sci.*, 56, 159–167, 1976. With permission.) (c) Dispersions of Laponite CP (0.2% by weight). (From R. Perkins, R. Brace, and E. Matijević, *J. Colloid Interf. Sci.*, 48, 417–426, 1974. With permission.)

- Laponite, 10 mmol/l (pH $\approx$ 8.5 (?) [7]); 2–20 mmol/l (pH increasing from 7 to 12 [119]; Figure 8.14(c)).

The data assembled above reveal the modest influence of the different types of montmorillonites; even beidellite and Laponite give c_K values similar to montmorillonites. As a function of pH, the c_K of sodium montmorillonite in the presence of salts showed a plateau between pH = 4 and 6 or 7 and increased at higher pH (Figure 8.14(b)) [110,117–119]. The dispersion coagulated spontaneously at pH<3.5 and was destabilized by the base necessary to rise the pH above 10.5. The c_K of Laponite increased linearly with pH (Figure 8.14(c)). A stepwise increase was also found for sodium kaolinite and $NaNO_3$, but not for sodium kaolinite and $Ca(NO_3)_2$ and $La(NO_3)_3$ (Figure 8.14(a)). Below pH = 6 the dispersions were destabilized by heterocoagulation between edges (+) and faces (−), and the critical coagulation concentration was very low. Recharging of the edges increased c_K of sodium montmorillonite from about 2 to 10 mmol/l $NaNO_3$. Coagulation may then occur by edge(−)–face(−) contacts. The importance of this type of contacts for the coagulation of pyrophyllite (no layer charge, only pH dependent edge charges) was clearly established [39]. It is also conceivable that band-like aggregates form with small contact areas between the faces. Coagulation by face–face contacts operating over large contact areas requires much higher salt concentrations.

The c_K values of Laponite CP at pH 7–10 were below the c_K values of the montmorillonite. The charge density of the Laponite layers is distinctly lower and probably negative edge charges gradually arise in the stronger alkaline medium only. As Laponite is very sensitive to acids, the dispersion could not be adjusted to pH below 7.

When sodium diphosphate is added to the dispersions, preferential binding of $H_2PO_4^-$ and HPO_4^{2-} ions by ligand exchange increases the edge charge density to a level that the salt concentration required to coagulate the dispersion by edge(−)/face(−) contacts approaches the value for face(−)–face(−) coagulation.[1] For instance, the c_K of NaCl for sodium

[1] In a similar way adsorption of the anionic surfactant sodium dodecylsulfate increased the C_K of NaCl to 136 mmol/liter at 10^{-1} mol/l surfactant [121].

montmorillonite dispersions increased to about 200 mmol/l when 0.1 mmol/l $Na_4P_2O_7$ was added [120]. The c_K value remained in the same order of magnitude when the concentration of diphosphate was increased (Table 8.4). As the area between two faces is much larger than between an edge and a face, coagulation occurs by face–face contacts. Keren et al. [117] suggested that face(−)–face(−) aggregation between two platelets is initiated by surface regions that, due to the charge heterogeneity (Section II.D, E), have lower specific charge densities than the average value of the montmorillonite surface.

Typical values of face–face coagulation are 0.25–0.30 *M* NaCl for beidellite, 0.33–0.38 *M* NaCl for montmorillonite from Cyprus, and 0.36–0.44 *M* NaCl for montmorillonite from Wyoming [115,122]. The more highly charged layers of beidellite (average surface charge density $\sigma_0 = 0.13$ C/m^2) are coagulated at distinctly lower NaCl concentrations than the montmorillonitic layers ($\sigma_0 = 0.10$ C/m^2). This is a consequence of the different charge distribution. Most of the negative charges in the layers of the beidellite are produced by the Al

Table 8.4 Effect of diphosphate addition on the critical NaCl concentration c_K of sodium beidellite dispersions (fraction 0.1–2 μm, 0.025% (w/w) beidellite) [115] and of polyphosphate addition on sodium montmorillonite (Wyoming) dispersions [116]

Beidellite			Montmorillonite	
$Na_4P_2O_7$ added (mmol/liter)	pH	c_K (mmol NaCl/l)	$NaPO_3$ added (mmol/l)	c_K (mmol NaCl/l)
0	6	6	0	12
1.25	6	230[a]	0.01	20
5.0	8.3	250[b]	0.1	80
10.0	9	270	1.0	120[b]
12.5	9.3	280		
25.0	9.7	310		

[a] Sodium montmorillonite dispersion at 0.1 mmol/l $Na_4P_2O_7$: $c_K = 195$ mmol NaCl/l [120].

[b] 0.1% (hydrogen, sodium) montmorillonite dispersion with 50 μmol $(NaP0_3)_6$/g montmorillonite: $c_K = 100$ mmol/l NaCl at pH = 2; $c_K = 200$–250 mmol/l NaCl at pH = 4; $c_K = 350$–400 mmol/l NaCl at pH = 8 [129].

for Si substitution and are therefore located in the tetrahedral sheets near the faces of the layer. The charges in montmorillonite created by substitutions and defects in the octahedral sheet are centered in the middle of the silicate layer. Thus, a larger number of counterions will reside in the Stern layer around the beidellite particles. Beidellite behaves as a colloidal particle with a constant surface charge density of about 0.07 C/m^2 [115].

Coagulation of sodium montmorillonite with other than sodium as counterions showed the same trend with increasing pH as for $NaNO_3$ (Figure 8.14(b)). As expected, the c_K values of $CsNO_3$ were considerably lower than for $NaNO_3$. The critical concentrations of monovalent cations for dispersions of Laponite were in a strange order (Figure 8.14(c)).

The visual determination of coagulation concentrations [79,120,123] requires very diluted dispersions (< 0.025%). The c_K values of more highly concentrated sodium montmorillonite dispersions (< 2%) could be derived from viscosity measurements. The salt concentration at which the viscosity steeply increased was considered to be the critical coagulation concentration [124]. Noteworthy is the increase of the c_K values of most salts with the solid content [124,125]. It is the consequence of counterion adsorption in the Stern layer [123,126,127]. In the presence of phosphates, however, the c_K of the 2% sodium montmorillonite dispersion was smaller than for the 0.025% dispersion [125].

B. Calculation of Interaction Energies

The interaction energy between the dispersed particles of clay minerals with alkali metal ions as counterions is calculated in terms of the DLVO theory. As the charge density of the faces is determined by the isomorphous substitutions and defects within the layer, the calculations are started under the assumption that the charge density of the faces remains constant at variable salt concentrations. This may be done in an easy way by the method of van Olphen [79].

Lubetkin et al. [128] measured the pressure created by several alkali montmorillonites and beidellites as a function of

the distance between the plates (calculated from the mass content of smectite assuming that the particles are completely delaminated) (Figure 8.15(a)). At separations above 5 nm the repulsive pressure arose solely from electrostatic repulsion. On the basis of diffuse layer interactions reasonably good agreement between theory and experiment was obtained (Figure 8.15(b)). The curves were calculated for a constant potential of $\psi = 150\,\text{mV}$ or in case of constant charge for $\sigma_0 = 0$ $0.118\,\text{C/m}^2$ (which is slightly above the typical charge density of Wyoming montmorillonite). The calculations did not take into account such factors as finite size of the ions and the particles and the charge heterogeneity. The silicate layers in the dispersion carry different charge densities, for Wyoming montmorillonite, for instance, varying between 0.08 and $0.12\,\text{C/m}^2$ (corresponding to interlayer cation densities of 0.24

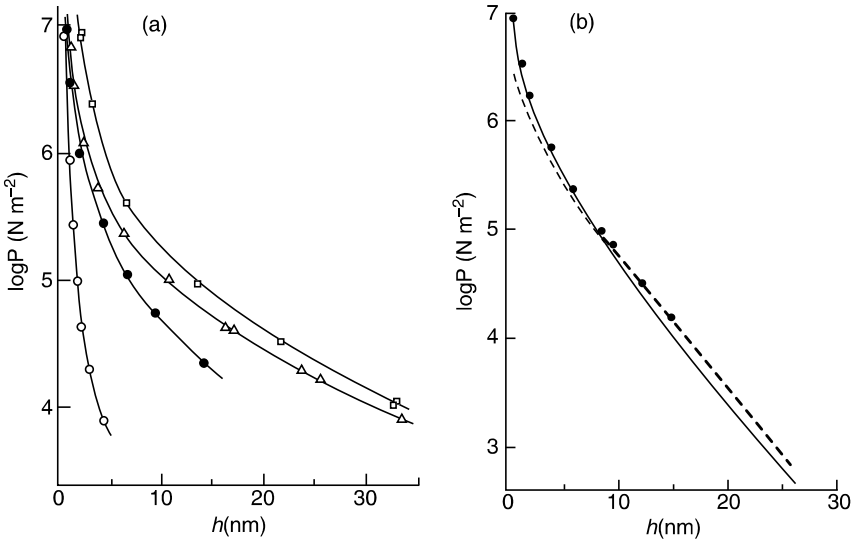

Figure 8.15 Pressure against plate distance h for Wyoming montmorillonite [128]. (a) In $10^{-4}M$ salt solutions of various counterions: □, Li^+; △, Na^+, ●, K^+, ○, Cs^+. (b) Experimental data for Li^+ montmorillonite in $10^{-2}M$ LiCl (●), and calculated curves for the constant potential model (---), constant surface charge model (—), and by approximate equation (Equation (7) in Ref. [128]) (. . . .).

and 0.34 eq/(Si, Al)$_4$ O$_{10}$). Ottewill [81] noted that the theory should be corrected for the fact that due to the finite volume of the dispersion a partition of the counterions between the clay dispersion and the external finite reservoir has to be considered.

The effect of tactoid formation is clearly seen in Figure 8.15(a). In the presence of alkali metal ions other than lithium and sodium ions the distances between the silicate layers are no longer equal; they are smaller within the tactoids than between the tactoids (Section III.C) and, therefore, the pressure decreases more strongly.

At separations of $\sim$1 nm the discontinuous decrease of the basal spacing indicates transition into the quasicrystalline structure. It is therefore no longer reasonable to calculate the interaction forces on the basis of the simple DLVO model. As discussed in Section III.B, the distribution of the interlayer cations differs considerably from that of two interacting double layers. The hydration shells around the interlayer cations resist further compression of the interlayer space.

Tombacz et al. [129] considered H^+-saturated montmorillonite as a solid acid with ionizable surface groups. They calculated the density of these sites and their intrinsic ionization constants from potentiometric and conductometric titrations [130,131]. Two groups of ionizable sites with intrinsic ionization constants $pK_{s1} = 2.6$ and $pK_{s2} = 6.4$ were distinguished. The total number of sites, $N_1 + N_2 = 4.8 \times 10^{17}$ (sites/m^2), was calculated from the cation exchange capacity of 0.59 meq/g (montmorillonite of Kuzmice, CSFR). The ratio of weak and strong acid groups was $N_2/N_1 = 0.41$, i.e., 29% of all sites were weak acidic centers. The most acidic sites were the H_3O^+ ions exchanged for the exchangeable sodium ions [34]. The surface potential as a function of pH was calculated from the charge densities. At $10^{-3}\,M$ NaCl and above pH 4, the surface potential showed a plateau at 185 mV. The surface potential decreased to 70 mV in $10^{-1}\,M$ NaCl and to 30 mV in $1\,M$ NaCl, and the plateau extended from pH $\approx$6. The total interaction curves (Hamaker constant $A = 0.5 \times 10^{-20}$ J) on the basis of these surface potentials were hypothetical at small distances (see remark above), but they clearly showed

that the maximum of the total interaction energy disappears at about 0.1 *M* NaCl (pH = 2), 0.3 *M* NaCl (pH = 4), and 0.4 *M* NaCl (pH = 8), which agrees with the experimental data (0.1 *M*, 0.2–0.25 *M*, and 0.35–0.40 *M* at pH = 2, 4, 8 [129] and 0.36–0.44 *M*, pH = 9 [115]).

A quite different (and for a colloid scientist strange) view was put forward by Low on the basis of extensive studies on the clay–water system. The hydration of the clay mineral surface was seen as the primary cause of swelling. This nonspecific interaction of water with the surfaces of clay particles could not be fully explained. Hydration of the interlayer cations was assumed to be of minor importance [82,83,132].

In contrast, Delville and Laszlo [62] showed that the Poisson–Boltzmann formalism correctly reproduces the relation between the interlamellar distance and the swelling pressure. The driving force is the stabilization of water molecules within the interlamellar force field. In all cases, the Poisson–Boltzmann approximation, modified to incorporate ion–polyion excluded volume effects, led to a concentration profile in agreement with Monte Carlo calculations. Recently, Quirk and Marčelja [133] examined published data for extensive swelling of Li^+-montmorillonite as revealed by $d_{(001)}$ spacings over the pressure 0.05–0.9 MPa and 1–10^{-4} *M* LiCl. The Poisson–Boltzmann theory and DLVO double-layer theory satisfactorily predicted surface separations over the range 1.8–12.0 nm. The DLVO theory with a 0.55 nm thick Stern layer indicated Stern potentials of -58 to -224 mV (for 1–10^{-4} *M* LiCl) and a constant Gouy plane charge of 0.038 C/m^2 (about 30% of the crystal lattice charge). There was no additional pressure contributed to hydration forces for surface separations of about 1.8 nm or larger. (However, the hydration force was considerable for muscovite with a surface charge density about three times that of montmorillonite [134].)

C. Coagulation of Dispersions Containing Two Smectites

The coagulation of dispersions containing differently charged particles was studied with colloidal smectites. When a disper-

sion of delaminated low and highly charged smectites is coagulated by addition of, for instance, sodium chloride, the particles can aggregate in different ways (Figure 8.16). When selective coagulation occurs, one sort of particles is formed first so that the coagulate consists of a mixture of crystals that contain the same layers as the starting crystals (but may differ in size and thickness). When low and highly charged layers aggregate within the individual crystals, mixed-layer crystals grow with random, regular, or zonal (segregation) layer sequences. The problem is to analyze the coagulate and find out which type of aggregation is predominant. The analysis is further complicated by the fact that the charge density varies to some extent within the individual crystals of the parent smectites (charge heterogeneity). There is only one method that allows a clear distinction between selective coagulation and random or regular mixed-layer formation. This

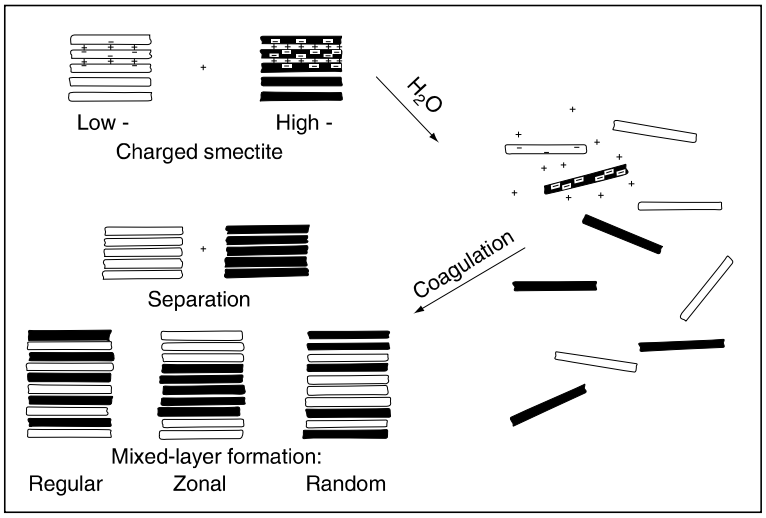

Figure 8.16 Disarticulation of sodium smectite crystals in water; formation of a colloidal dispersion and re-aggregation to crystals by coagulation (surface charges and interlayer cations not entirely shown). (From E. Frey and G. Lagaly, *J. Colloid Interf. Sci.*, 70, 46–55, 1979. With permission.)

is the measurement of the charge distribution by the alkylammonium ion exchange (Section II.E) [30,32,115,135].

Two differently charged smectites were used: a montmorillonite (Upton, Wyoming) with a mean surface charge density $\sigma_0 = 0.096\,\text{C/m}^2$ (mean interlayer cation density $\bar{\xi} = 0.192\,\text{C/m}^2$) and beidellite (Unterrupsroth, Germany) with $\sigma_0 = 0.13\,\text{C/m}^2$ ($\bar{\xi} = 0.26\,\text{C/m}^2$). The cation density in the interlayer spaces of the montmorillonite varied from 0.17 to $0.25\,\text{C/m}^2$ and of beidellite from 0.20 to $0.35\,\text{C/m}^2$ (Figure 8.17).

The homoionic sodium smectites were dispersed in $0.01\,M$ sodium diphosphate solution at pH > 7 to give dispersions with a mass content of 250 mg/l. Equal volumes of these

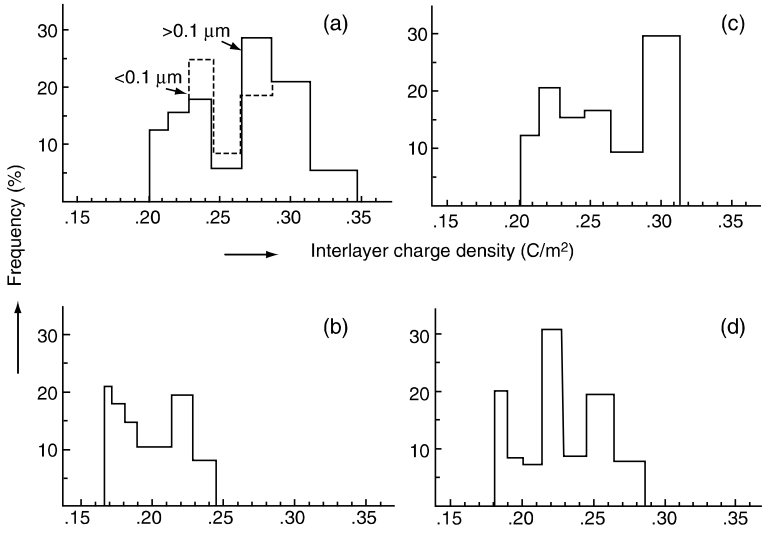

Figure 8.17 Formation of mixed-layer crystals by coagulation of dispersions containing two smectites. (a) Pure beidellite (Unterrupsroth, Germany; particle size fraction <0.1 μm and 0.1–2 μm). (b) Pure montmorillonite (Wyoming, USA; particle size fraction <2 μm). (c) Coagulated material from the mixed colloidal dispersion, particle size fraction 0.1–2 μm. (d) Coagulated material from the mixed colloidal dispersion, particle size fraction <0.1 μm. (From E. Frey and G. Lagaly, *J. Colloid Interf. Sci.*, 70, 46–55, 1979. With permission.)

colloidal dispersions were mixed and coagulated under different experimental conditions. The following results were obtained:

1. The type of aggregation was determined by the particle size and was less dependent on the experimental conditions.
2. Larger particles (fraction 0.1–2 μm) were selectively coagulated. Experimental conditions could be selected to separate beidellite from montmorillonite:
   a. Slow coagulation by adding NaCl solution gradually to rise the Na^+ concentration to 0.28 M, pH = 9. Coagulate: mostly beidellite-like particles, remaining dispersion: dispersed montmorillonite.
   b. Rapid coagulation by fast addition of NaCl, final concentration 0.5 M NaCl. Coagulate: mixtures of low and highly charged particles. As discussed in Section V.A, the beidellite coagulated at a lower salt concentration. The particles composed of low or highly charged layers were not identical to the particles of the starting materials. The charge distribution curve of the highly charged particles (Figure 8.17(c)) was substantially different from that of the starting beidellite particles (Figure 8.17(a)).
3. When the particles were smaller than 0.1 μm, the coagulate consisted of mixed-layer crystals. The charge distribution curve (Figure 8.17(d)) clearly proved that low and highly charged layers succeeded in the same crystal. The layer sequence was not completely random; swelling tests revealed a certain amount of segregated layers [135].

In Figure 8.18 is explained why only very small particles are mixed during coagulation. The maximum total interaction energy $V_{t,m}$ is calculated for particles of 10^2 and 10^4 nm^2 and surface charge densities 0.069, 0.096, and 0.12 C/m^2. The total interaction curves are obtained by the linear superposition approximation for constant surface charge density

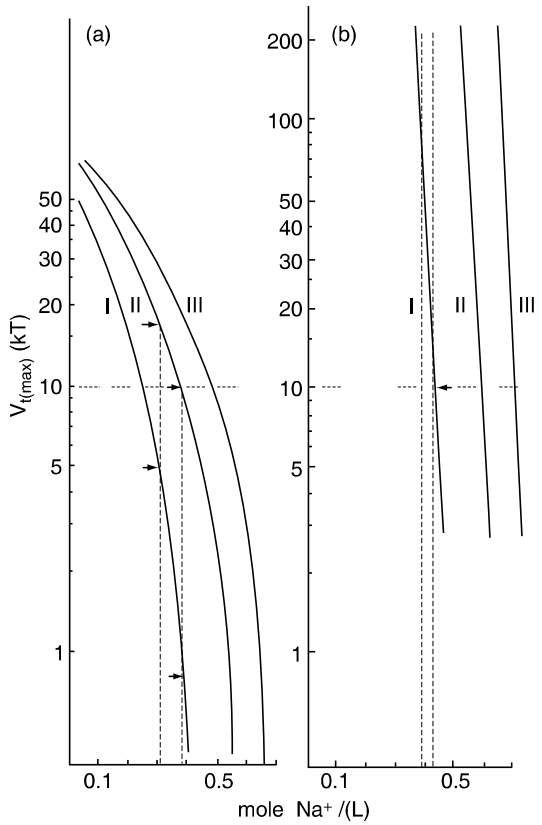

Figure 8.18 Maximum interaction energy (in kT/plate) as a function of Na^+ concentration for particles $10 \times 10\,nm^2$ (a) and $100 \times 100\,nm^2$ (b). Surface charge densities: I, 0.069; II, 0.096; III, $0.120\,C/m^2$; calculated for constant charge density, Hamaker value 5×10^{-20} J. (From E. Frey and G. Lagaly, *J. Colloid Interf. Sci.*, 70, 46–55, 1979. With permission.)

[79]. The curves are cut at half distances of 0.5 nm ($d_1 = 2\,nm$) because at smaller distances DLVO calculations are no longer appropriate. At $0.3\,M$ NaCl, $V_{t,m}$ is about $5\,kT$/particle for the small particles and $\sigma_0 = 0.069\,C/m^2$ (representative of beidellite) and $17\,kT$/particle for $\sigma_0 = 0.096\,C/m^2$ (montmorillonite) (Figure 8.18(a)). An increase of concentration to $0.38\,M$

NaCl leads to $V_{t,m} \approx 1\,kT$/particle for $\sigma_0 = 0.069\,C/m^2$ and $V_{t,m} \approx 10\,kT$/particle for $\sigma_0 = 0.096\,C/m^2$. Thus, mixing of both types of layer is highly probable during coagulation. The curves calculated for larger particles (Figure 8.18(b)) clearly reveal that, at a salt concentration of about $0.4\,M$, only the beidellitic layers are coagulated whereas $V_{t,m}$ of the montmorillonitic layers remains so high that coagulation is prevented.

It is interesting to consider the depth of the secondary minimum. For larger layers with low charge density the depth is about $50\,kT$/particle and it is $\approx 20\,kT$/particle for the more highly charged layers. Thus, aggregation of the low-charged layers is initiated by preliminary demixing in the secondary minimum.

In more sophisticated calculations, the total interaction energies have to be calculated between differently charged plates. This reduces $V_{t,m}$ and makes the mixing of the small particles still more probable [136,137]. For large particles, the differences of $V_{t,m}$ remain large enough to prevent the layers from mixing during coagulation. The effect of particle size on the simultaneous coagulation of differently charged particles is also evident from the calculations of Pugh and Kitchener [138].

The delamination of illite–smectite mixed-layer crystals was studied in detail [74,75]. At conditions of delamination, only the smectitic interlayer spaces expand largely, and the particles break asunder into *fundamental particles* consisting of one, two, or a few illitic layers (Figure 8.13, Section IV.D). The physical dimensions of the fundamental particles were determined by TEM techniques. Once the clay minerals had been fully disarticulated, mixed colloidal dispersions could be prepared which, after re-aggregation, produced illite–smectite mixed-layer crystals substantially different from the starting materials. Aggregation may be performed not only by coagulation but also by other methods like simple air-drying, spray drying, or freeze-drying. Some possible applications are directed to the design of special heterogeneous catalysts and the preparation of very thin films and coatings [139,140].

VI. FLOCCULATION AND STABILIZATION OF CLAY DISPERSIONS BY MACROMOLECULES

A. Flocculation by Polyanions

Polymers are extensively used as flocculating agents for clay dispersions. In practical applications, polyanions are more effective in flocculating clay dispersions than polycations. Polyanions are attached to the particles at a few sites, and larger parts of the macromolecules remain free in solution to form bridges between neighboring particles.

Several studies are reported on the adsorption of polyacrylates and polyacrylamides on montmorillonite [94,141,142] and on kaolinite [143–147]. Polyacrylates and hydrolyzed polyacrylamides are bound by complex formation between carboxylate groups of the polyanion and aluminum ions exposed at the edges. Thus, polyacrylate adsorption on sodium montmorillonite reaches a maximum at pH 7.

Polyamides, as a consequence of hydrolysis, often contain carboxylate groups, so that they may be attached at the edges like polyacrylates. In addition, two further binding mechanisms between the clay mineral surface and the amide groups are operative:

1. *Hydrogen bonds between the amide groups and aluminol and silanol groups at the edges of kaolinite particles*. It seems that formation of these hydrogen bonds is competitive with hydrogen bond formation between neighboring surface OH groups (aluminol and silanol groups). Thus, hydrogen bonding of polyacrylamide to silanol groups as anchoring sites is promoted when, in acidic medium, neighboring aluminol groups are protonated. In alkaline medium, bonding to aluminol groups is favored, when the neighboring silanol groups are dissociated. The amount of polyacrylamide adsorbed by kaolinite therefore goes through a minimum at pH 6–8 [144,146].
2. Polyamide groups are protonated by the increased acidity of the interlayer water molecules of smectites and then bound by electrostatic forces [141].

The addition of polyacrylamide to sodium kaolinite dispersions (2% by mass) initiated different types of aggregation [148]. The fraction of flocculated kaolinite decreased first to a minimum, then increased to a maximum (Figure 8.19). Polyacrylamide that was adsorbed at the edges broke up edge(+)–face(−) contacts and increased the dispersibility of the kaolinite particles (B→C in Figure 8.19).[2] Bridging of the particles by the macromolecules at somewhat higher levels of polyacrylamide addition (C→E) increased the amount of flocculated kaolinite, which at high dosages of polymer again was reduced by steric stabilization (E→F). The floc density (determined from sediment volume and weight after freeze drying) changed in inverse direction to the amount flocculated. The presence of polymer on the edges of the particles prevented the formation of extended networks during sedimentation, and the particles were more densely packed (C in Figure 8.19). Bridging produced more loosely packed flocs (E in

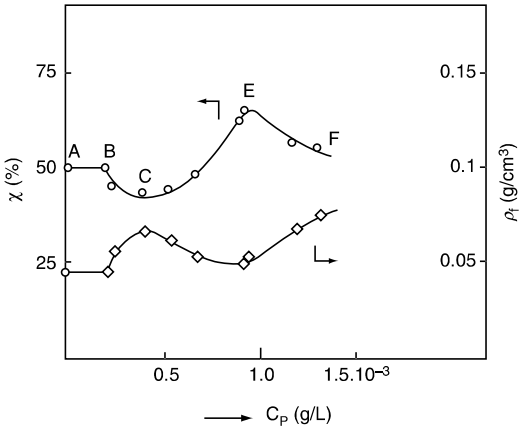

Figure 8.19 Flocculation of sodium kaolinite dispersions (2% by weight) with polyacrylamide ($M = 1.2 \times 10^6$) in $10^{-4}\,M$ NaCl (concentration c_P) at pH = 3.7. ○, fraction χ of kaolinite flocculated; ◇, density ρ_f of the flocs [148].

[2] On the edges of kaolinite particles pronounced adsorption of polyacrylamides was in fact observed [149].

Figure 8.19). The increase of floc density from E to F revealed that the most loosely packed aggregates were first redispersed by steric stabilization.

Bottero et al. [142] studied the effect of polyacrylamide on dispersions of sodium montmorillonite. The polyacrylamide did not flocculate montmorillonite particles but influenced the structure of the tactoids.

B. Flocculation by Polycations

Polycations are strongly adsorbed, and many segments are attached to the negative surface, so that bridging between particles does not occur as easily as in the presence of polyanions. In many cases flocculation occurs as a consequence of charge neutralization. This type of flocculation often requires a sophisticated adjustment of clay, polymer and salt concentration, and pH [150].

Durand–Piana et al. [151] examined the effect of cationic groups attached to polyacrylamide on the flocculation of sodium montmorillonite dispersions. Random copolymers of m units acrylamide (AM) and n units N,N,N-trimethyl aminoethyl chloride acrylate (CMA) were synthesized:

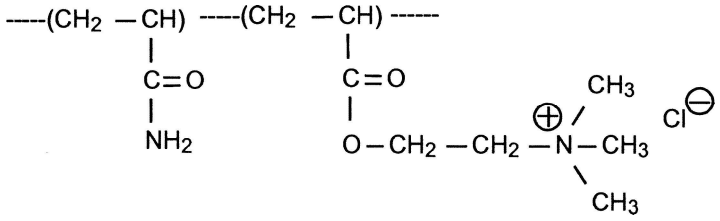

The cationicity $\tau = n/(n+m)$ was varied between 0 and 1. At low cationicities flocculation occurred by bridging of the particles by the weakly charged polyelectrolytes. The optimal flocculation concentration decreased with increasing molecular mass and, for $\tau \geq 0.01$, with increasing cationicity. Above ≥ 0.2 flocculation seemed to occur by charge neutralization, and the optimal flocculation concentration became independent of the molecular mass (Figure 8.20). It is interesting to note that the saturation value of adsorption decreased with the

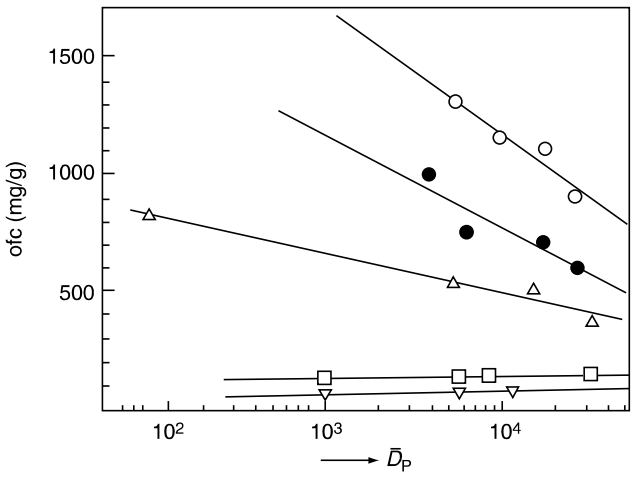

Figure 8.20 Optimal flocculation concentration (ofc, mg/g sodium montmorillonite) versus degree of polymerization, $\overline{D}_p$, for polycations (see formula) of various cationicities τ: ○, $\tau = 0.01$; ●, $\tau = 0.05$; Δ, $\tau = 0.13$; □, $\tau = 0.30$; ▽, $\tau = 1.0$ [151].

montmorillonite concentration when the solid content exceeded 2 g/l. Aggregation of montmorillonite platelets is strong enough to limit the surface area available to polymer adsorption.

Due to the opposite charges polycations penetrate into the interlayer spaces to a certain extent. However, an increasing number of contacts are formed between their positive centers and the surface charges that retard and eventually stop the diffusion of the polycations between the layers. However, complete coverage of the interlamellar surfaces by polycations may be achieved by a similar disaggregation–reaggregation process as proposed for the lysozym adsorption on sodium montmorillonite [152]. When a tactoid, in which the external faces are saturated with the polycations, collides with another tactoid, which has no polycations on its faces, strong interaction between the polymer-covered face and the bare face can peel an individual layer off the either tactoid. Thus, two fresh surfaces are exposed for further interaction

with polycations. Eventually, all layers are aggregated interleaved with polycations, and form thick particles [153,154].

Parazak et al. [155] studied flocculation of dispersed montmorillonite, kaolinite, illite, and silica by three types of polycations: poly(dimethylamine epichlorohydrin), poly (dimethyl diallylammonium chloride), and poly(1,2-dimethyl-5-vinylpyridinium chloride). The results were interpreted in terms of *hydrophobic interactions*. The idea was that adsorbed polycations, their charges neutralized, are considered as hydrophobic moieties. Contact between these hydrophobic patches of two approaching particles will induce flocculation by hydrophobic interaction, even if only a part of the particle charges are neutralized by the polycations.

In papermaking cationic lattices (*polymer microparticles*) were introduced as flocculants to improve retention, drainage, and formation (*retention aids*) [156]. In other two-component microparticle retention systems cationic polyacrylamide and bentonite particles induce the deposition of the calcium carbonate particles on fiber surfaces. The montmorillonite particles form bridges between the fiber and calcium carbonate particles, both covered with the polycations. Therefore, conditions such as prolonged or intense mixing that cause delamination of thicker montmorillonite particles can lead to detachment and subsequent flocculation of the polyamide coated carbonate particles [157].

C. Peptization (Deflocculation) of Clays by Macromolecule

As seen in the previous section, optimal flocculation is reached at distinct polymer concentrations (Figure 8.20). At larger polymer dosages restabilization occurs, and the amount of flocculated clay decreases again. Restabilization is accompanied by an increased salt stability. A very instructive example was reported by van Olphen [79] (Figure 8.21). Addition of CMC (sodium carboxy methylcellulose) to a sodium bentonite dispersion first decreased the critical NaCl concentration from 20 mmol/l to 10 mmol/l (sensitizing action of CMC), and then increased the colloidal stability strongly up to 3.5 mol/l. Steric stabilization is the main cause of the enhanced salt stability.

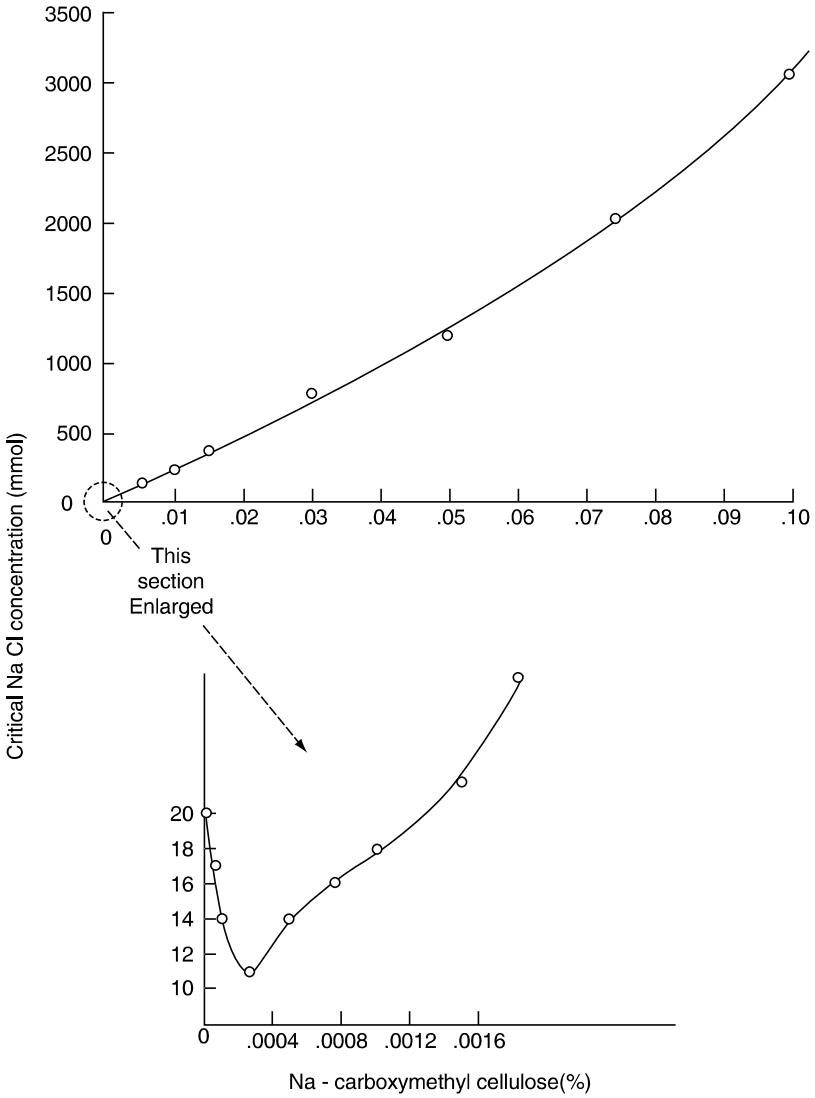

Figure 8.21 Effect of sodium carboxy methylcellulose on the salt stability of sodium bentonite dispersions [79].

The effect of polymer addition seen in Figure 8.21 is basically different from the action of several other polyanions like natural tannates (Figure 8.22(a)). The addition of very small amounts of Quebracho tannate increased the critical salt concentration strongly to a plateau at 270 meq/l NaCl. This polyanion does not exert steric stabilization but simply acts by recharging the edges. Because tannate is added as sodium salt, the total amount of sodium ions in the dispersion increases to 430 meq/l at the highest dosage of tannate (dotted line in Figure 8.22(a)). This range of the critical counterion concentration is typical of face–face aggregation of clay mineral particles (Section V.A).

Polyphosphate ions belong to the most important deflocculants in practical applications (Section VIII.A). In the presence of polyphosphate, the critical coagulation concentration of NaCl increased to a maximum and decreased with further addition of the polyanion (Figure 8.22(b)). However, the total concentration of sodium ions increased only slightly at higher amounts of polyphosphate (≥ 200 meq/l) and is, again, typical of face–face aggregation.

VII. AGGREGATION OF CLAY MINERAL PARTICLES AND GELATION

A. Types of Aggregation

The most popular is the model of house of cards where the clay mineral particles are held together by edge–face contacts [158–160] (Figure 8.23(a)). However, this type of network only forms when the edges are positively charged or in slightly alkaline medium above critical salt concentrations. The formation of edge–face contacts below pH ≈ 6 is a heterocoagulation between the positive edges and the negative faces of the particles or silicate layers. Establishment of card-houses results in non-Newtonian flow of the dispersions and development of yield stresses in the slightly acidic medium (Figure 8.24 and Figure 8.25). Note the yield value increasing with temperature at pH $= 4.5$. The formation of the card-house

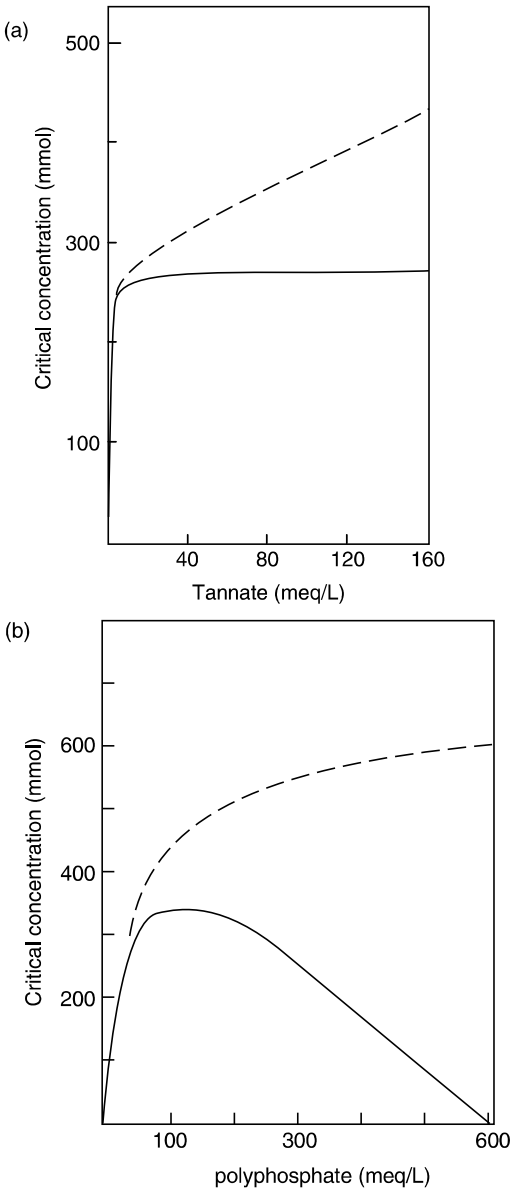

Figure 8.22 Effect of polyanions on the salt stability of sodium bentonite dispersions [50]. —, critical NaCl concentration to attain coagulation; - - -, total Na^+ concentration at the point of coagulation. (a) Quebracho tannate (sodium salt). (b) Sodium polyphosphate [79].

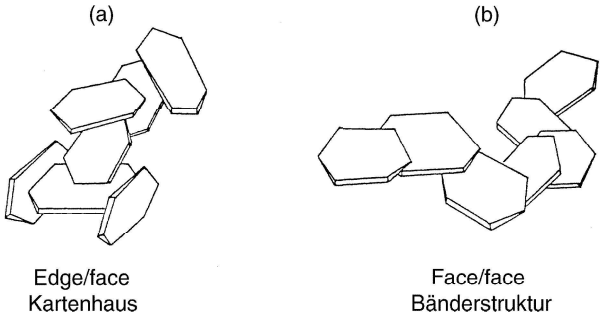

Figure 8.23 Aggregation of clay mineral platelets in (a) card-house and (b) band-type networks by edge–face and face–face contacts.

structure is one of the main causes of plasticity of ceramic masses [158,159].

With increasing pH the network composed of edge–face contacts breaks down and, in the rheological experiments, the shear stress τ (at a given rate of shear, $\dot{\gamma}$) of the sodium montmorillonite dispersion decreases to a sharp minimum (Figure 8.25). The increase in the shear stress at pH >5 results from the higher degree of delamination and, therefore, from the higher number of particles in the dispersion. Raising the pH above 7 requires increased amounts of NaOH, which reduce the degree of delamination and the electroviscous effect [161] (Section VII.C), and the shear stress decreases again. The maximum of the shear stress at pH $\sim$7 disappears in the presence of calcium ions which impede the delamination of the particles (Figure 8.25) [121].

Weiss and Frank [162,163] first stressed the importance of face–face contacts and the possibility of formation of three-dimensional band-type networks (*Bänderstrukturen*) (Figure 8.23(b)). The band-type network of calcium kaolinite was found to show some elasticity in contrast to the more rigid card-house structure.

The addition of calcium ions has a pronounced effect on the type of aggregation. As discussed in Section III.D, calcium ions held together the silicate layers at maximum distances of

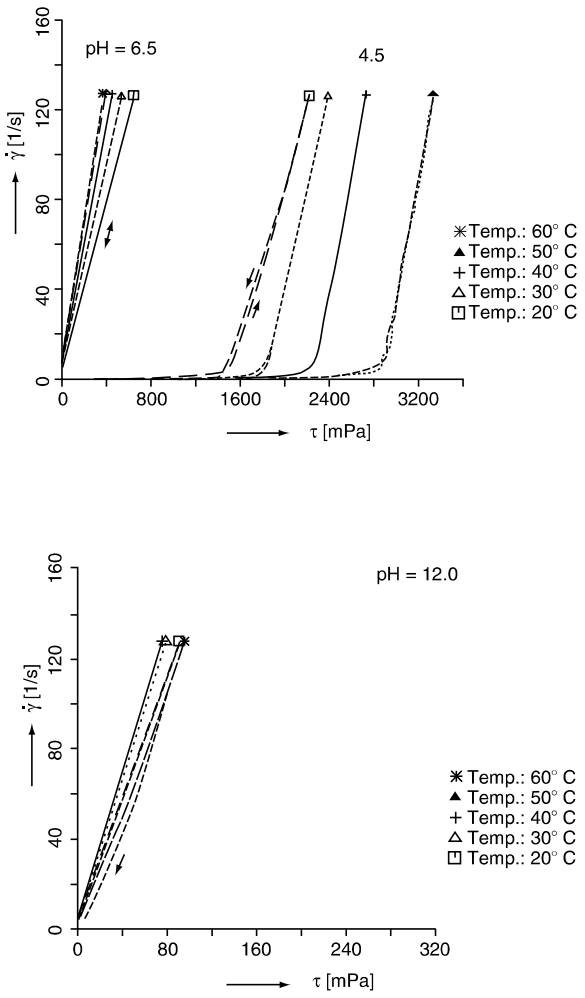

Figure 8.24 Flow curves (shear rate $\dot{\gamma}$ versus shear stress τ) for sodium montmorillonite dispersions (Wyoming, 4% by weight) at various pH values and different temperatures (pH adjusted by addition of HCl or NaOH).

1 nm (basal spacing 2 nm). Even small amounts of calcium ions nucleate face–face contacts and build up band-type networks. The flow behavior of Ca/Na–bentonite dispersions

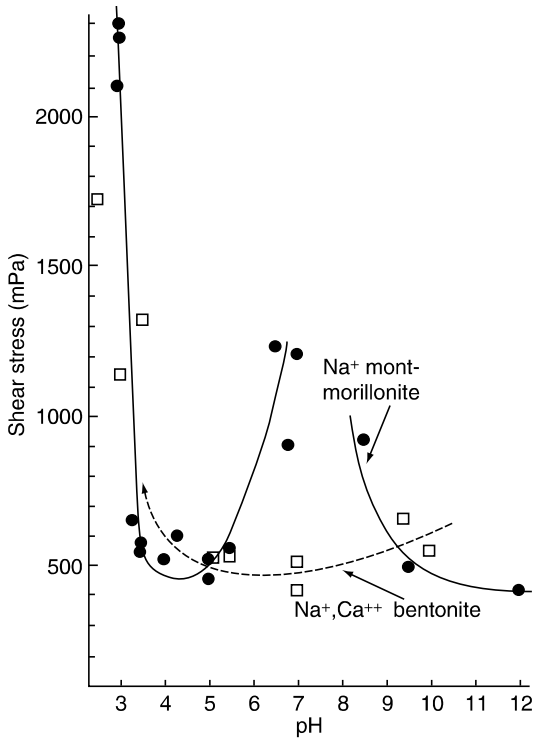

Figure 8.25 Dependence of the shear stress (at $\dot{\gamma} = 94.5\ s^{-1}$) on the pH value for the sodium montmorillonite dispersion (from Wyoming, M 40; ● —) and the dispersion of the parent sodium calcium bentonite (□ - - - -). The pH values were determined with indicator sticks just before the rheological measurements. (From T. Permien, G. Lagaly, *Clays Clay Miner.*, 43, 229–236, 1995. With permission.)

is, therefore, complex and depends sensitively on the ratio of Ca/Na in the dispersion [164]. Small amounts of calcium ions added to a sodium montmorillonite dispersion promote face–face contacts and stabilize band-type networks (Figure 8.26(b)). At larger amounts of calcium ions, the bands are contracted to smaller aggregates and, eventually, particle-like assemblages, and the network break asunder (Figure 8.26(c)). Thus, homoionic calcium smectites show only a modest tendency of formation of band-type networks.

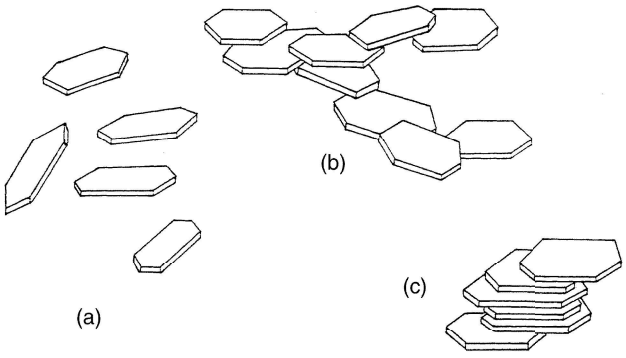

Figure 8.26 Modes of aggregation in the presence of calcium ions: (a) single platelets or silicate layers, (b) band-type aggregates, (c) compact *crystals*.

It may be assumed that calcium ions held between the negative charges at the edges and faces of two approaching particles act in a similar way as in the interlayer space and limit the particle distance to 2 nm. Stable edge(−)–Ca^{2+}–face(−) contacts would then be created which would build up a stable card-house network. However, I consider this behavior very unlikely. Calcium ions lying at the edges of particles with very irregular contour lines are in a quite different force field than between the planar silicate layers in the interlayer space. The modest importance of the edge(−)–Ca^{2+}–face(−) contacts is expressed by the low shear stresses of the calcium montmorillonite dispersions in alkaline medium.

B. Sedimentation, Filtration

In many practical applications (Chapter 8) sedimentation and type of the sediments play an important role. Figure 8.27 shows highly dispersed clay mineral plates and two types of aggregates. The sediments or filter cakes formed from these dispersions are substantially different. Highly peptized dispersions of individual platelets (or silicate layers) form virtually impermeable filter cakes and compact, dense sediments that are difficult to stir. The formation of filter cakes

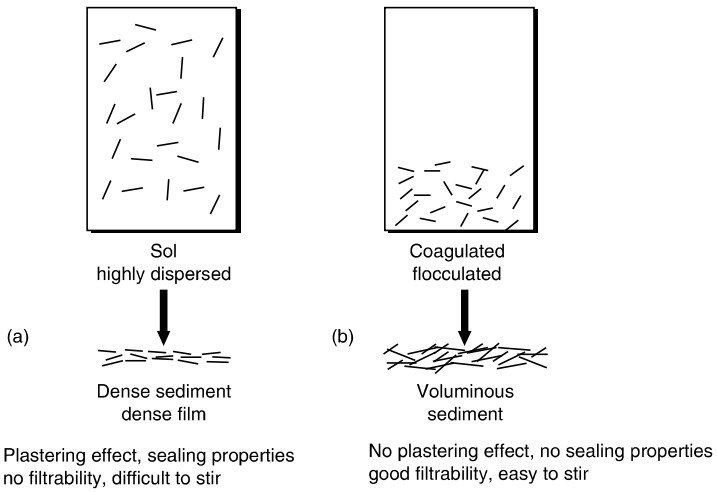

Figure 8.27 Structure and properties of sediments formed from well dispersed (a) and aggregated (b) particles.

finds many applications in sealing operations and causes the plastering effect of drilling muds (Section VIII.B). It is of great importance in producing ceramic casts (Section VIII.A).

The compact sediments or filter cakes form if the interaction between the particles is repulsive. When the particle–particle interaction becomes attractive, the particles aggregate to some extent, and voluminous sediments are formed with large pores between the clay mineral plates. These sediments are easy to redisperse by stirring and show no plastering effect. In the simplest way settling of the particles and properties of the sediments are adjusted by the Na^{+}/Ca^{2+} ratio (Section VII.A). Dispersions of calcium montmorillonite showed an unusual settling behavior [165].

The influence of bentonite content, pH, and pressure on the permeability of filter cakes was thoroughly studied by Benna et al. [166,167]. The effect of the aggregation of the clay mineral platelets on the filterability was clearly established.

C. Sol–Gel Transitions

The transition from a sol into a gel and vice versa is very important in many practical applications (Chapter 8). Gels are usually described as dispersed systems, which show certain stiffness so that, for instance, the vessel containing the dispersion can be turned without the dispersion flowing out. Gels show certain elasticity, and we used creeping measurements to distinguish between sol and gel [168].

The experiment is shortly explained in Figure 8.28. When a constant shear stress τ_e is applied to the dispersion within time t_e, the strain increases as shown. At $t = t_e$ the shear stress is set to zero, the sample relaxes and in case of a viscoelastic behavior, the strain decreases to a plateau. If the dispersion is a viscous fluid, the strain increases further. The reversible part of the compliance ($J = \gamma/\tau_0$) is $J_{rev} = 100\ (J_0 + J_R)/(J_0 + J_R + J_N)$. The position of the plateau gives the elastic $(J_0 + J_R)$ and viscous (I_N) contribution to the compliance. A sol shows $J_{rev} = 0$, a gel $J_{rev} > 0$.

Figure 8.29 shows the reversible compliance of a sodium montmorillonite dispersion as a function of the NaCl concentration. $J_{rev} > 0$ indicates gel formation at low- and high-salt concentrations. Stiffening at low-salt concentration results

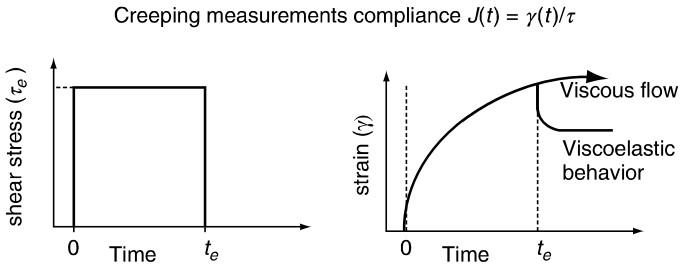

Figure 8.28 Creeping experiments: The strain (relative deformation) γ is shown as a function of time t. During the time t_e the sample is deformed by applying the constant shear stress τ_e. At $t = t_e$, τ is set to zero and the sample relaxes (viscoelastic behavior, full line) or flows further (viscous fluid). (From S. Abend and G. Lagaly, *Appl. Clay Sci.*, 16, 201–227, 2000. With permission.)

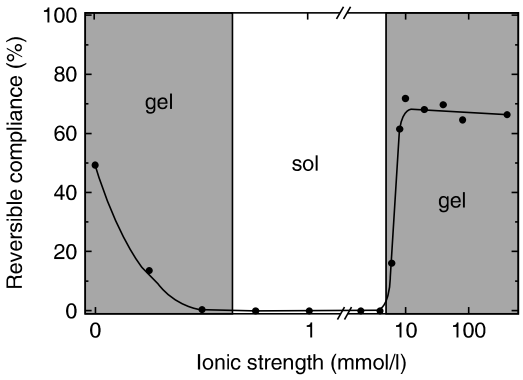

Figure 8.29 Reversible compliance as a function of the NaCl concentration. The 4% (w/w) dispersion of sodium montmorillonite (M 50, Ordu Turkey). (From S. Abend and G. Lagaly, *Appl. Clay Sci.*, 16, 201–227, 2000. With permission.)

from the electroviscous effect (Figure 8.30) [161]. At these conditions the single silicate layers, lamellae, or packets of them are surrounded by the diffuse layers of counterions and are repelled from each other by electrostatic forces [2,79,123,133,169]. When the particle concentration is sufficiently high ($\geq 1\%$ (w/w) for many sodium montmorillonite dispersions). The diffuse ionic layers around the silicate layers, lamellae, or packets restrict the translational and rotational motion of these units. The thin shape of these units is seen as a critical factor for the appearance of the electroviscous effect [170]. The consequence is a certain parallel orientation of the platelets (see Ref. [168]). The dispersion stiffens and becomes gel-like above 3–3.5% (w/w) montmorillonite. This type of gel is called *repulsive gel* (not correctly because the interparticle force, and not the gel, is repulsive). The addition of salt reduces the thickness of the diffuse ionic layer, the particle become again more mobile, and the gel turns into a sol.

The principles of the structure of sodium smectite gels were derived from small-angle scattering experiments of synchrotron beam [171]. A sodium smectite gel (Wyoming montmorillonite, 20 g in 100 g water $\equiv$ 17% (w/w) montmoril-

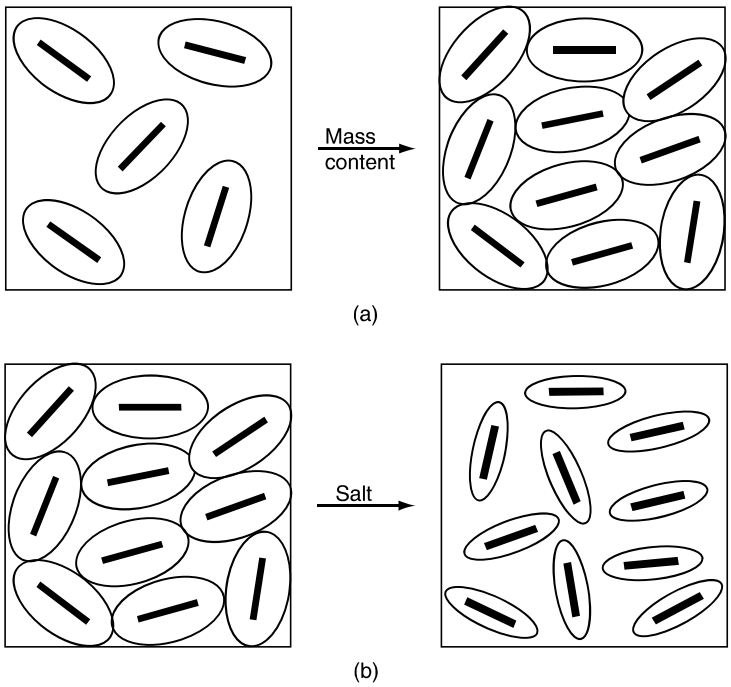

Figure 8.30 The electroviscous effect: (a) Sufficiently high-particle concentration reduces the mobility of the particles. (b) When the thickness of the diffuse ionic layers decreases at higher salt concentration, the particles again become more mobile.

lonite) was studied before and after several cooling–heating cycles between $-70^{\circ}C$ and room temperature. Below $-10^{\circ}C$ the silicate layers were aggregated to thick particles (500–600 nm thick) which were composed of domains of four to five silicate layers in regular distances with two water layers in between. These domains were separated by zones of one or two silicate layers spaced less regularly by one, three, or four layers of water. During heating to room temperature the interlamellar spaces took up water molecules to form the discrete hydrates with up to four water layers. This process proceeded slowly and could be followed by the changes in the scattering patterns. The insertion of more than four water layers was accompanied by a dramatic expansion of the inter-

layer space to form a gel in which assemblages of (in an average) four to five almost parallel silicate layers (with $d_{001} \approx 8$ nm) were still retained. Isolated silicate layers filled the space between these units and the domains of four to five layers, and the single layers were no longer parallel. About 25% of the layers were distributed as single layers. An interesting point is that the domains of four to five layers (in distances of about 8 nm) reflected the structure of the particle in the frozen gels. As the changes during cooling–heating cycles were nearly reversible, the deviation of the silicate layers from parallel orientation during heating must be modest, say, by no more than 15°. Several causes of this peculiar behavior were mentioned [50]. At the same water content the number of layers in the domains was specific of the mineral. An interesting influence of the charge distribution in beidellite gels was noted. The layers constituting the domains remained at spacings of 1.54 nm and did not move in distances of 7–8 nm as in montmorillonite, saponite, and hectorite [50]. Organization of the layers at different levels was also observed in TEM and small-angle x-ray scattering (SAXS) studies [172,173].

Gel formation at higher salt concentration, above the critical coagulation concentration, is caused by attractive forces between the particles when the van der Waals attraction dominates the electrostatic repulsion (*attractive gel*). At lower salt concentration the interaction is attractive between edges(−) and faces (−), at higher concentrations it becomes also attractive between the faces. Likely, there is a continuous transition from the edge(−)–face(−) (card-house) to the face(−)–face(−) aggregation (band-type structure). If the forces between the faces are strongly attractive at high-salt concentration, the network is contracted and disrupted (Figure 8.23(b) and (c)). Distinct particles form, the dispersion destabilizes and forms flocs which settle into a sediment.

Attractive gels often show thixotropic behavior. In this case the gel is liquefied by shaking, stirring, or pouring but stiffens again with time. Stiffening and liquefaction are strongly reversible. The cause is a network of weakly adhering particles. When mechanical energy is applied, particle

contacts are broken, and the network is disintegrated into many fragments. When resting, the fragments driven by the Brownian motion of the solvent molecules came into contacts again forming an extended network, and the liquefied dispersion becomes gel-like. This reversible process requires attraction, but not too strongly attractive particle–particle interactions. Thixotropy is a very important property in many practical applications of clay, kaolin, and bentonite dispersions (Chapter 8).

The domains of sol, repulsive gel, attractive gel, and flocs are clearly seen in the phase diagrams for two sodium montmorillonites (Figure 8.31). The large domain of sol separates the two types of gels. As expected, the repulsive gel only forms when the particle concentration is >3% (w/w) and 3.5% (w/w), respectively. The salt concentration at which the gel liquefies into the sol increases with the particle concentration because more densely packed particles require thinner diffuse ionic layers to become mobile again. In the case of attraction between the particles, the attractive gel is also built-up at smaller solid contents because band-type aggregates can span a distinctly larger volume. Flocs are only formed at the highest salt concentration and not at too high particle concentrations. When sodium ions are replaced by potassium and cesium ions, the attraction between the particles becomes stronger because these counterions are more strongly adsorbed in the Stern layer. The band-type aggregates are more stable and resist to floc formation. A 2% (w/w) sodium montmorillonite dispersion does not coagulate forming flocs even at the highest KCl and CsCl concentrations, but remains in the state of the gel (Figure 8.32). The liquefying action of phosphate addition [125] is also seen in the sol–gel diagram (Figure 8.32). This effect is also very pronounced for kaolinite dispersions (see Figure 8.34) [125].

D. Hydrogels of Organoclays

Garett and Walker [174,175] first described formation of gels of low-charged vermiculites in water when the inorganic counterions are replaced by butylammonium ions. The gels

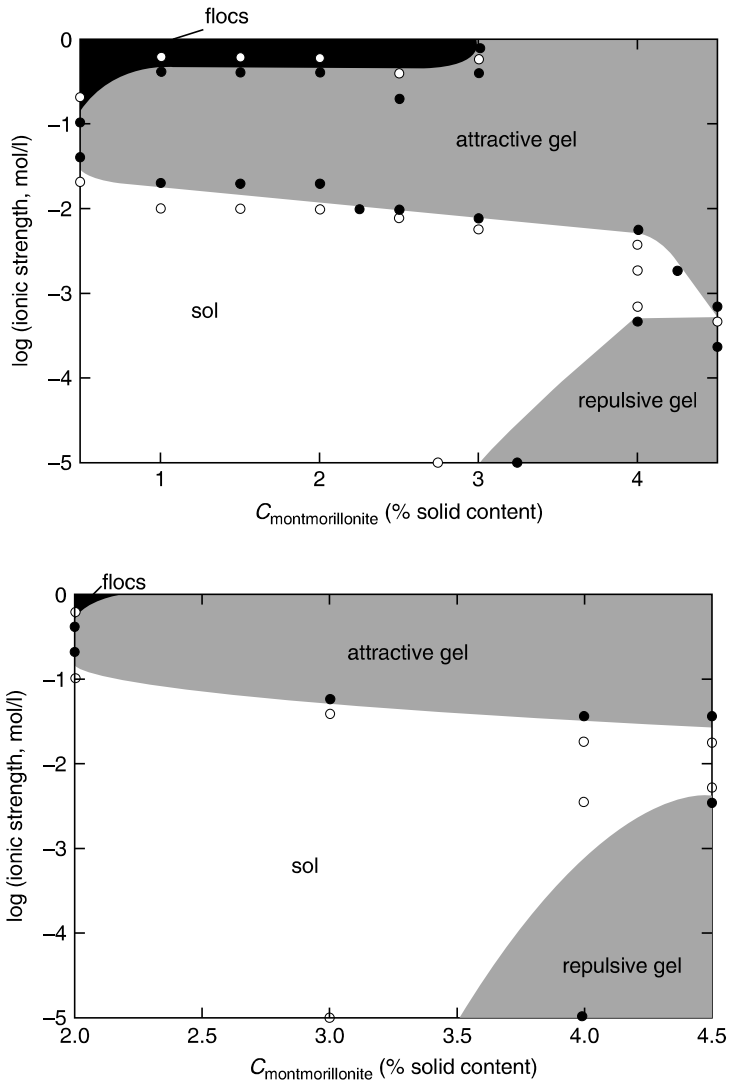

Figure 8.31 Sol–gel diagram for sodium montmorillonite and NaCl. (a) montmorillonite of Ordu, Turkey (M 50); (b) montmorillonite of Wyoming (M 40A). (From S. Abend and G. Lagaly, *Appl. Clay Sci.*, 16, 201–227, 2000. With permission.)

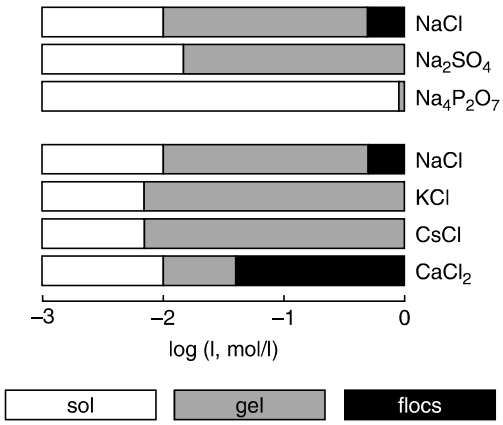

Figure 8.32 Effect of a few salts on the transitions sol–gel and gel–flocs. The 2% (w/w) sodium montmorillonite (Ordu, Turkey, M 50), I = ionic strength. (From S. Abend and G. Lagaly, *Appl. Clay Sci.*, 16, 201–227, 2000. With permission.)

are formed as a consequence of the delamination of the butylammonium vermiculite crystals [176–180]. This very peculiar behavior seems to be related to the organization of the water molecules between the alkyl chains [181]. It is evident that the swelling of the butylammonium vermiculites cannot be described by the DLVO theory because hydrophobic interactions also have to be considered. In a quite different model, Smalley and co-workers discussed the swelling and gel formation of butylammonium vermiculite on the basis of the Coulombic attraction theory (Sogami theory) and postulated the existence of long-range attraction between the vermiculite layers [182,183].

Rausell-Colom and Salvador [184,185] described gel formation of vermiculites in solutions of amino acids like γ-aminobutyric acid, ω-aminocaproic acid, and ornithine. The repulsion between the carboxylate groups accumulated in the interlayer spaces promotes the delamination of the particles. The gels are composed of independently diffracting large packets of several silicate layers (19 layers spaced around $d = 13.5$ nm; Santa Ollala vermiculite in the presence

of 2×10^{-2} mol/l ornithine, confined by a pressure of 99.4 g/cm^2). These packets have an average thickness of 260 nm, and they are completely separated from each other by the solution phase. Within the packets, ordered coherent domains (with about six silicate layers in equal distances of 13.1 nm) are separated by layers also in parallel orientation but less regularly spaced [186].

Stable colloidal dispersions of fully delaminated montmorillonites were obtained by exchanging the inorganic interlayer cations by betaines $(CH_3)_3\ N^+-(CH_2)_n-CO_2^-\ Li^+$ (Na^+). These dispersions were more stable against salts than Li^+ and Na^+ montmorillonite (LiCl: $c_K = 60$ and 50 mmol/l for $n = 7$ and 11). Very high LiCl concentrations (>1 mol/l) were needed to coagulate the betaine derivatives ($n > 5$) in the presence of diphosphate [35].

E. Gelation in Organic Solvents

Thickening of organic solvents by hydrophobized bentonites (in a few cases also clays and kaolins) is needed in many practical applications [2,187]. Gelation of these dispersions often requires small amounts of polar additives (water, ethanol) to increase the gel strength [2,188–190]. This effect was explained by the strong orientation of the adsorbed water molecules, which creates giant dipole moments on the particles and hydrogen bonds between the particles [189].

In referring to practical applications the following effect must be noted. In an industrial scale organophilic bentonites usually are prepared by reacting the bentonite with quaternary alkylammonium ions without removing an excess of these cationic surfactants. The presence of these excess amounts can sensitively influence the flow behavior of dispersions in organic solvents (Figure 8.33). The 1% dispersion of a technical dimethyl dioctadecylammonium bentonite in xylene (activated with 0.2% ethanol and 0.02% water) showed low shear stress values ($\tau = 400$ mPa at $\dot{\gamma} = 130\ s^{-1}$). The excess surfactant cations adsorbed by the particles enhanced the electrostatic repulsion, acting like a lubricant between the particles. When these cations were removed by washing, the dispersion

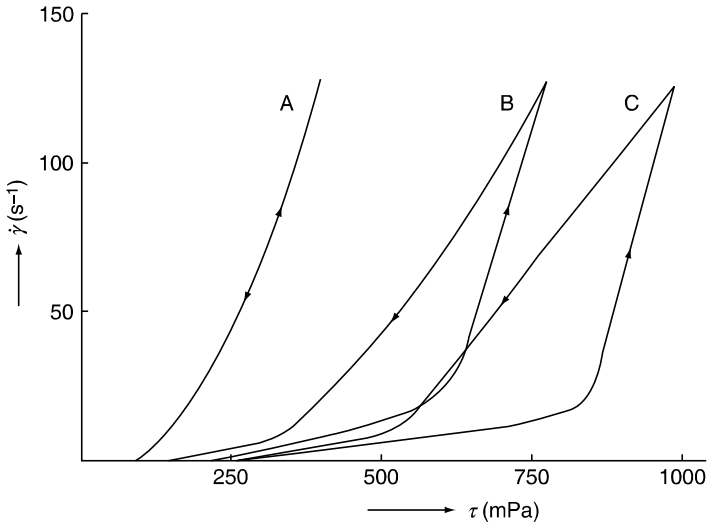

Figure 8.33 Flow behavior (rate of shear $\dot{\gamma}$ against shear stress τ) of a 1% (w/w) dispersion of dimethyl dioctadecylammonium bentonite in xylene containing 0.2% ethanol and 0.02% water. (a) Organo bentonite as obtained with an excess of the alkylammonium salt (1.22 mmol N/g bentonite); (b) after washing out the excess of the alkylammonium salt (1.02 mmol N/g bentonite); (c) again exchanged with alkylammonium ions with the excess of the salt carefully removed (1.33 mmol N/g bentonite). (From K. Jasmund and G. Lagaly, Eds., *Tonminerale und Tone: Struktur, Eigenschaften, Anwendung und Einsatz in Industrie und Umwelt*, Steinkopff Verlag, Darmstadt, 1993, pp. 1–490. With permission.)

stiffened and showed pronounced thixotropy. This example shows that even small changes in the ratio surfactant/bentonite can distinctly change the flow properties and the thixotropic (or antithixotropic) behavior.

VIII. APPLICATIONS

A. Common Clays and Kaolins

Ceramic masses contain 25–55% (by mass) of common clay and, for porcelain production, kaolins. Their plastic properties

are brought about by the interactions between the clay mineral particles, predominantly by edge(+)–face(−) contacts. Ceramic bodies are produced by manual or mechanical shaping, in the simplest way on a potter's wheel, or by pouring a deflocculated slip (with solid contents up to 72% by mass) into plaster molds. A filter cake builds up on the inside surface of the mold which finally is dried and fired. The final properties of the deposited particle layers depend on the state of aggregation of the dispersion and a delicate balance between coagulation or flocculation and peptization has to be maintained to achieve the optimum properties of the final product.

To make the ceramic mass sufficiently fluid, the card-house-type interactions between the plates must be broken by the addition of deflocculants. Deflocculant addition must be carefully adjusted and should be less than the amount required for optimum deflocculation (cf. Ref. [3]). For instance, a plastic mass containing about 70% by mass kaolin is *liquefied* by 0.3% tetrasodium diphosphate (*pyrophosphate*) at pH = 8. The dispersion can be easily poured when freshly made. Figure 8.34 very nicely demonstrates the effect of diphosphate addition on a kaolin slurry. Increased face–face attraction after addition of 3 g KCl again stiffens the dispersion.

Other deflocculants are sodium salts of inorganic or organic polyanions such as polyphosphates, water glass, and polyacrylates. Dispersions produced by polyphosphate addition become unstable with time, probably because of the formation of complex aluminum phosphates. Some kaolin slurries in the presence of polyphosphate form gels that can give discharge problems. The addition of polyacrylate reduces the risk of gelation [4].

The deflocculating agents are strongly adsorbed at the edges. In acidic medium, they recharge the edges from positive to negative or, at somewhat higher pH, increase the negative charge density. Due to ligand exchange reactions (Figure 8.3) these anions also are bound around the neutral point and in slightly alkaline medium. The edge (+)–face(−) contacts are eliminated, and the card-house structure is no longer stable. Adjusting pH to ≈8 supports the effect of re-

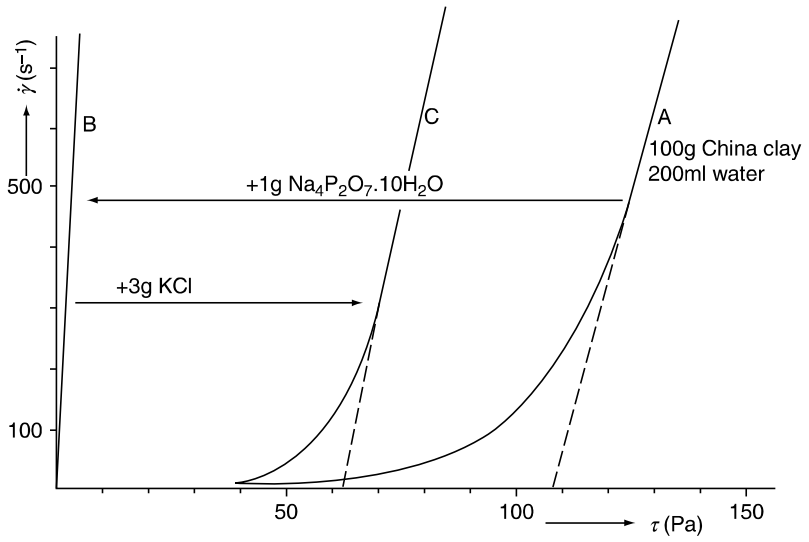

Figure 8.34 Liquefaction of 100 g kaolin in 200 ml water by addition of 1 g tetrasodium diphosphate, $Na_4P_2O_7 \cdot 10\ H_2O$ (A → B) and stiffening of the liquefied kaolin by addition of 3 g potassium chloride (B → C). (Courtesy of Professor Dr. M. Müller–Vonmoos, ETH Zurich; see also Ref. [38]).

charging by the deflocculants. The deflocculating agents also have to keep the calcium and magnesium ions in solution (or, in some cases, to precipitate them) because otherwise these ions would increase the viscosity by initiating face(−)–face(−) and edge(−)–face(−) contacts [38].

The use of kaolins as fillers and coating pigments in the production of paper requires a very strong control of the rheological properties. In paper coating the coating color (a mixture of the deflocculated kaolin and an adhesive) is applied at shear rates as high as $10^6\,s^{-1}$. The important variables that govern the flow properties are not only type and concentration of the deflocculants [149] but also kaolinite particle size, shape, and packing [4].

B. Bentonite Dispersions

Colloidal bentonite dispersions find many important applications. In civil engineering the dispersions are wanted for a variety of uses [2,3]. For slurry walling a thixotropic bentonite dispersion is used as an intermediate supporting material, which obviates the need for any revetting. Only sodium bentonites or soda-activated bentonites can be used which show a significant level of thixotropy. The formation of a thin impermeable filter cake of clay mineral plates on the walls prevents excessive loss of fluid to the surrounding formation (plastering effect).

The second, very important practical application of bentonites is for use in drilling fluids [2,3,79]. About 2.5 million tons of bentonite were required in 1982 for the preparation of drilling muds. The smectites in these dispersions have to act in different ways. During the drilling operation the impermeable filter cake built up by the clay mineral plates on the wall of the hole prevents the loss of fluid into the formation. The drilling fluid is circulated to bring the drill cuttings up and to cool the bit efficiently. When the drilling operation is interrupted before the drill cuttings and sand have been circulated out of the hole, the setting of the cuttings and sand particles is prevented by thixotropic stiffening. In offshore drilling or in drilling through salt domes the mud must be protected against destabilization by salts. A further problem arises from the large increase in viscosity of common drilling muds at elevated temperatures. Hectorite-type minerals were specially formulated to resist high temperatures for drilling deep wells and geothermal areas.

The properties that are most significant in the abovementioned uses are dispersibility, viscosity, yield value, thixotropy, and good plastering effects. Only natural sodium bentonites or certain sodium-exchanged calcium bentonites have these necessary properties. In practice, a compromise often must be obtained between the different requirements. For instance, development of thixotropic drilling muds requires conditions, which are adverse to an optimum of plastering and pumping properties. Thus, many types of organic and inorganic additives are used to regulate the behavior of the muds.

Stability against salts is obtained by addition of nonionic or anionic polymers (modified starches, sodium carboxymethyl cellulose, tannates) (see also Section VI.C).

Quebracho tannates (Figure 8.22(a)) are the peptizing agents in the *red muds*. The large increase of viscosity in deeper holes can be shifted to higher temperatures by the addition of solid calcium or barium hydroxide. The addition of calcium ions is somewhat contradictory in view of the powerful coagulating action of the divalent metal ions. Complexing of the calcium ions by tannate reduces their coagulating effect. A certain degree of face–face aggregation still occurs, as the particles in the fine red muds are thicker than in the red muds.

The *surfactant muds* provide an interesting example of a dispersion which is in coagulated state but which still shows the properties required for drilling fluids at a reasonable level. Surfactant muds contain polyoxyethylene-type nonionic polymers, polyanions such as sodium carboxymethyl cellulose, and strongly coagulating electrolytes such as calcium sulfate.

In the practical uses described above, natural sodium bentonites (e.g., bentonite from Wyoming) or calcium bentonites converted to the sodium form have to be selected. Natural sodium bentonites generally contain some amounts of calcium ions (sometimes also magnesium ions). Soda activation consists of reacting natural calcium bentonites with soda. The amount of sodium ions added corresponds to about the ion exchange capacity. As the calcium ions are not removed from the system, optimal delamination is not reached (and also not wanted in many practical applications). When about 1 meq soda/g bentonite is added, the interlayer calcium ions are only partially replaced by sodium ions. Increasing amounts of soda displace progressively the interlayer calcium ions. Calcium ions that are not precipitated as $CaCO_3$ promote face–face contacts. The shear stress (at a given shear rate) as a function of the amount of soda added increases to a maximum value at 2–5 meq soda/g bentonite (Figure 8.35) [38]. The increasing shear stress results from the progressive delamination which is accompanied by formation of band-type networks, predominantly with face(−)−Ca^{2+}–face(−) contacts. At very high concentrations of soda higher amounts of calcium ions are

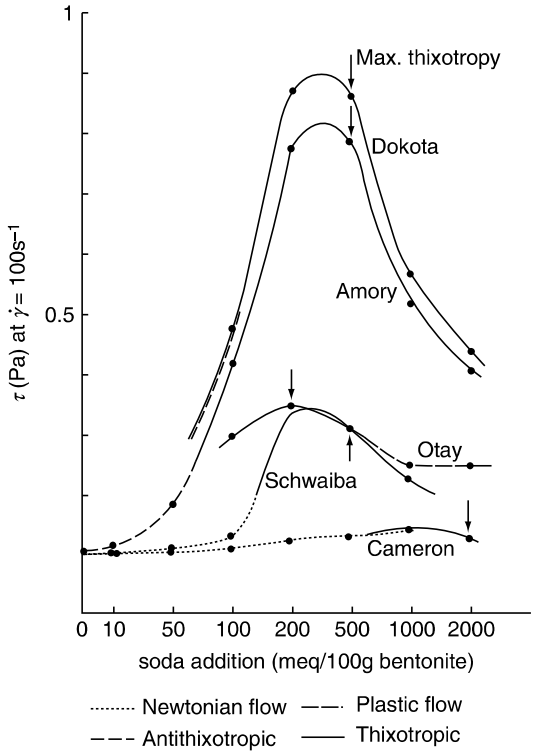

Figure 8.35 Effect of soda addition on the flow behavior. The 2% (w/w) dispersion of several bentonites. The arrows indicate the point of maximum thixotropy (maximum hysteresis in the flow curves. . . . Newtonian flow, – · – · – · – plastic flow; – – – – antithixotropic behavior; ——— thixotopic behavior. (From G. Lagaly, *Appl. Clay Sci.*, 4, 105–123, 1989. With permission.)

precipitated and are withdrawn from the face–face contact areas. The network breaks down and the shear stress decreases from the maximum to a low value.

IX. FINAL REMARKS

Many scientists reject the study of clay dispersions. They consider clays as dirty materials, mixtures of minerals and

consisting of particles of irregular shape. A few scientists and users arrive at a positive attitude and then are fascinated by the variety and variability of the reactions of the different clay minerals. The same is true for colloid scientists: the first contacts with clay dispersions can be disgusting, but further acquaintance produces fascination. The variety of properties discussed above and the variety of practical applications have no parallel compared to other colloidal systems.

REFERENCES

1. G. Lagaly and R. Fahn, in *Ullmann's Encyclopedia of Technical Chemistry*, 4th ed., Vol. 23, Verlag Chemie, Weinhein, 1983, pp. 311–326.
2. K. Jasmund and G. Lagaly, Eds., *Tonminerale und Tone: Struktur, Eigenschaften, Anwendung und Einsatz in Industrie und Umwelt*, Steinkopff Verlag, Darmstadt, 1993, pp. 1–490.
3. I.E. Odom, *Philos. Trans. R. Soc., London A*, 311, 391–409, 1984.
4. W.B. Jepson, *Philos. Trans. R. Soc., London A*, 311, 411–432, 1984.
5. B.S. Neumann and K.G. Sansom, *J. Soc. Cosmet. Chem.*, 21, 237–258, 1970.
6. B.S. Neumann and K.G. Sansom, *Israel J. Chem.*, 8, 315–322, 1970.
7. B.S. Neumann and K.G. Sansom, *Clay Miner.*, 9, 231–243, 1971.
8. J.D.F. Ramsay, *J. Colloid Interf. Sci.*, 109, 441–447, 1986.
9. R.G. Avery and J.D.F. Ramsay, *J. Colloid Interf. Sci.*, 109, 448–454, 1986.
10. J.T. Kloprogge, S. Komarneni, and J.E. Amonette, *Clays Clay. Miner.*, 47, 529–554, 1999.
11. K.A. Carrado, *Appl. Clay Sci.*, 17, 1–23, 2000.
12. T. Kodama, Y. Harade, M. Ueda, K. Shimizu, K. Shuto, S. Komarneni, W. Hoffbauer, and H. Schneider, *J. Mater. Chem.*, 11, 1222–1227, 2001.
13. J.T. Kloprogge, *J. Porous Mater.*, 5, 5–41, 1998.
14. G.W. Brindley and G. Brown, Eds., *Crystal Structures of Clay Minerals and Their X-ray Identification*, Mineralogical Society, London, 1980.

15. R.T. Martin, S.W. Bailey, D.D. Eberl, D.S. Fanning, S. Guggenhein, H. Kodama, D.R. Pevear, J. Środoń, and F. Wicks, *Clays Clay Miner.*, 39, 333–335, 1991.
16. S.P. Altaner and R.F. Ylagan, *Clays Clay Miner.*, 45, 517–533, 1997.
17. D.D. Eberl, R. Nüesch, V. Sucha, and S. Tsipursky, *Clays Clay Miner.*, 34, 185–191, 1999.
18. D.M. Moore and R.C. Reynolds, *X-ray Diffraction and the Identification and Analysis of Clay Minerals*, 2nd ed., Oxford University Press, Oxford, 1997, pp. 1–378.
19. A. Plançon, *Clay Miner.*, 36, 1–14, 2001.
20. H. Vali and H.M. Köster, *Clay Miner.*, 21, 827–859, 1986.
21. C. Chenu and A.M. Jaunet, *C.R. Acad. Sci., Paris 30*, Series 2, 1990, pp. 975–980.
22. O. Touret, C.H. Pons, D. Tessier, and Y. Tardy, *Clay Miner.*, 25, 217–233, 1990.
23. G. Lagaly and R. Malberg, *Colloids Surf.*, 49, 11–27, 1990.
24. J. Benbrahin, N. Armagau, G. Besson, and C. Tschoubar, *Clay Miner.*, 21, 111–124, 1986.
25. H. Suquet and H. Pézérat, *Clays Clay Miner.*, 35, 353–362, 1987.
26. C. Tschoubar, A. Plancon, J. Benbrahin, C. Clinard, and C. Sow, *Bull. Miner.*, 105, 477–491, 1982.
27. G. Lagaly, *Clays Clay Miner.*, 27, 1–10, 1979
28. J. Cuadres and J. Linares, *Clays Clay Miner.*, 43, 467–473, 1995.
29. M. Müller-Vonmoos, G. Kahr, and F.T. Madsen, in *Identifizierung und Nachweis der Tonminerale*, H. Tributh and G. Lagaly, Eds., Berichte der DTTG, Giessen, 1990, pp. 131–155.
30. G. Lagaly, *Clay Miner.*, 16, 1–21, 1981.
31. G. Lagaly, *Clays Clay Miner.*, 30, 215–222, 1982.
32. G. Lagaly, in *Layer Charge Characteristics of 2:1 Silicate Clay Minerals*, A.R. Mermut, Ed., CMS Workshop Lectures, Vol. 6, The Clay Mineral Society, Boulder, CO, USA, 1994, pp. 1–46.
33. D.C. Bain and B.F.L. Smith, in *A Handbook of Determinative Methods in Clay Mineralogy*, M.J. Wilson, Ed., Blackie, Glasgow, 1987, pp. 248–274.
34. M. Janek and G. Lagaly, *Appl. Clay Sci.*, 19, 121–130, 2001.
35. C.U. Schmidt and G. Lagaly, *Clay Miner.*, 34, 447–458, 1999.
36. M.R. Böhmer and L.K. Koopal, *Langmuir*, 8, 2649–2665, 1992.
37. U. Brandenburg and G. Lagaly, *Appl. Clay Sci.*, 3, 263–279, 1988.

38. G. Lagaly, *Appl. Clay Sci.*, 4, 105–123, 1989.
39. R. Keren and D.L. Sparks, *Soil Sci. Soc. Am. J.*, 59, 430–435, 1995.
40. B.K.G. Theng, *The Chemistry of Clay Organic Reactions*, A Hilger, London, 1974.
41. G. Lagaly, *Philos. Trans. R. Soc. A*, 311, 315–332, 1984.
42. G. Lagaly, in *Developments in Ionic Polymers*, Vol. 2, A.D. Wilson and H.J. Prosser, Eds., Elsevier, London, 1986, pp. 77–140.
43. G. Lagaly, Proceedings of the International Clay Conference, L.G. Schultz, H. von Olphen, and F.A. Mumpton, Eds., Clay Mineral Society, Bloomington, IN, 1987, pp. 343–351.
44. P.M. Costanzo, R.F. Giese, and C.V. Clemency, *Clays Clay Miner.*, 32, 29–35, 1984.
45. P.M. Costanzo and R.F. Giese, *Clays Clay Miner.*, 38, 160–170, 1990.
46. Y. Komori, Y. Sugahara, and K. Kuroda, *Chem. Mater.*, 11, 3–6, 1999.
47. P.G. Slade, J.P. Quirk, and K. Norrish, *Clays Clay Miner.*, 39, 234–238, 199.
48. G. Frens and J.Th.G. Overbeek, *J. Colloid Interf. Sci.*, 38, 376–387, 1972.
49. J.Th.G. Overbeek, *J. Colloid Interf. Sci.*, 58, 408–422, 1977.
50. C.H. Pons, E. Rousseaux, and D. Tschoubar, *Clay Miner.*, 17, 327–338, 1982.
51. A. Weiss, A. Häbisch, and A. Weiss, *Ber. Dtsch. Keram. Ges.*, 41, 687–690, 1964.
52. H. Suquet, C. de la Calle, and H. Pézérat, *Clays Clay Miner.*, 23, 1–9, 1975.
53. J. Hougardi, W.E.E. Stone, and J.J. Fripiat, *J. Chem. Phys.*, 64, 3840–3851, 1976.
54. G. Besson, C. Mifsud, D.D. Tschoubar, and J. Mering, *Clays Clay Miner.*, 22, 379–384, 1974.
55. R. Glaeser, I. Mantin, and J. Mering, *Bull. Groupe Fr. Arg.*, 19, 125–130, 1967.
56. J. Mamy and J.P. Gaultier, Proceedings of the International Clay Conference, Mexico, Applied Pub. Ltd., Wilmette, III, 1975, pp. 149–155.
57. C. Poinsignon, J.M. Cases, and J.J. Fripiat, *J. Phys. Chem.*, 82, 1855–1860, 1978.
58. R.F. Giese and J.J. Fripiat, *J. Colloid Interf. Sci.*, 71, 441–450, 1979.

59. J.J. Fripiat, J. Cases, M. Francois, and M. Letellier, *J. Colloid Interf. Sci.*, 89, 378–400, 1982.
60. J.J. Fripiat, M. Letellier, and P. Levitz, *Philos. Trans. R. Soc., London A*, 311, 287–299, 1984.
61. C.T. Johnston, G. Sposito, and C. Erickson, *Clays Clay Miner.*, 40, 722–730, 1992.
62. A. Delville and P. Laszlo, *New J. Chem.*, 13, 481–491, 1989.
63. M.M. Mortland and K.V. Raman, *Clays Clay Miner.*, 16, 393–398, 1968.
64. P. Touillaux, P. Salvador, C. Vandermeersche, and J.J. Fripiat, *Israel J. Chem.*, 6, 337–348, 1968.
65. S.S. Cady and T.J. Pinnavaia, *Inorg. Chem.*, 17, 1501–1507, 1978.
66. I. Grandjean and P. Laszlo, *Clays Clay Miner.*, 37, 403–408, 1989.
67. D.J. Mulla and P.F. Low, *J. Colloid Interf. Sci.*, 95, 51–60, 1983.
68. F.R.C. Chang, N.T. Skipper, and G. Sposito, *Langmuir*, 13, 2074–2082, 1997.
69. F.R.C. Chang, N. Skipper, and G. Sposito, *Langmuir*, 11, 2734–2741, 1995.
70. N.T. Skipper, G. Sposito, and F.R.C. Chang, *Clays Clay Miner.*, 43, 285–293, 294–303, 1995.
71. F.R.C. Chang, N.T. Skipper, and G. Sposito, *Langmuir*, 14, 1201–1207, 1998.
72. J.A. Greathouse, K. Refson, G. Sposito, *J. Am. Chem. Soc.*, 122, 11459–11464, 2000.
73. J. Norris, R.F. Giese, P.M. Costanzo, and C.J. van Oss, *Clay Miner.*, 28, 1–11, 1993.
74. P. Nadeau, *Clay Miner.*, 20, 499–514, 1985.
75. J. Środoń, D.D. Eberl, and V.A. Drits, *Clays Clay Miner.*, 48, 446–458, 2000.
76. L.L. Schramm and J.C.T. Kwak, *Clays Clay Miner.*, 30, 40–48, 1982.
77. K Norrish, *Disc. Faraday Soc.*, 18, 120–134, 1954.
78. J.D. Cebula, R.K. Thomas, and J.W. White, *J. Chem. Soc. Faraday I*, 76, 314–321, 1980.
79. H. van Olphen, *An Introduction to Clay Colloid Chemistry*, John Wiley and Sons, New York, 1977.
80. L.M. Barclay and R.H. Ottewill, *Spec. Disc. Faraday Soc.*, 138–147, 1970.
81. R.H. Ottewill, *J. Colloid Interf. Sci.*, 58, 357–373, 1977.

82. Y. Sun, H. Lin, and P.F. Low, *J. Colloid Interf. Sci.*, 122, 556–564, 1986.
83. P.F. Low, Proceedings of the International Clay Conference, Denver, 1985, L.G. Schultz, H. van Olphen, and F.A. Mumpton, Eds., Clay Minerals Society, Bloomington, IN, 1987, pp 247–256.
84. C.J. van Oss, R.F. Giese, and P.M. Costanzo, *Clays Clay Miner.*, 38, 151–159, 1990.
85. R.D. Fitzsimmons, A.M. Posner, and J.P. Quirk, *Israel J. Chem.*, 8, 301–314, 1970.
86. W.B. Kleijn and J.D. Oster, *Clays Clay Miner.*, 30, 383–390, 1982.
87. R. Kjellander, S. Marčelja, and J.P. Quirk, *J. Colloid Interf.* Sci., 126, 194–211, 1988.
88. R. Kjellander, *Ber. Bunsenges Phys. Chem.*, 100, 894–904, 1996.
89. O.P. Mehra and M.L. Jackson, *Clays Clay Miner.*, 7, 317–327, 1960.
90. G.G.S. Holmgreen, *Soil Sci. Soc. Am. Proc.*, 31, 210–211, 1967.
91. M.S. Stul and L. van Leemput, *Clay Miner.*, 17, 209–215, 1982.
92. H. Tributh and G. Lagaly, *GIT Fachz. Lab.*, 30, 524–529, 771–776, 1986.
93. V.C. Farmer and B.D. Mitchell, *Soil Sci.*, 96, 221–229, 1963.
94. B. Siffert and P. Espinasse, *Clays Clay Miner.*, 28, 381–387, 1980.
95. J.K. Anderson, *Clays Clay Miner.*, 10, 380–388, 1963.
96. B.D. Mitchell and B.F.L. Smith, *J. Soil Sci.*, 25, 239–241, 1974.
97. W.D. Keller, *Clays Clay Miner.*, 26, 1–20, 1978.
98. W.D. Keller and R.P. Haenni, *Clays Clay Miner.*, 26, 384–396, 1978.
99. W.D. Keller, *Clays Clay Miner.*, 33, 161–172, 1985.
100. A. Weiss, *Angew. Chem.*, 72, 755–762, 1963.
101. N. Lahav, *Clays Clay Miner.*, 38, 219–222, 1990.
102. R. Grim and N. Güven, *Bentonites: Geology, Mineralogy and Uses*, Elsevier, New York, 1978.
103. W.D. Keller, R.C. Reynolds, and A. Inoue, *Clays Clay Miner.*, 34, 187–197, 1986.
104. L.A. Pérez-Maqueda, O.B. Caneo, J. Poyato, and J.L. Pérez-Rodriguez, *Phys. Chem. Miner.*, 28, 61–66, 2001.
105. M. Janek, P. Komadel, and G. Lagaly, *Clay Miner.*, 32, 623–663, 1997.

106. U. Schwertmann, Proceedings of the International Clay Conference, Tokyo, 1969, Israel University Press, Jerusalem, 1969, pp. 683–690.
107. I. Barshad, *Soil Sci.*, 108, 38–42, 1969.
108. H.R. His and D.F. Clifton, *Clays Clay Miner.*, 9, 269–275, 1962.
109. B.G. Williams and S.P. Drover, *Soil Sci.*, 104, 326–331, 1967.
110. L.S. Swartzen-Allen and E. Matijević, *J. Colloid Interf. Sci.*, 56, 159–167, 1976.
111. H. Jenny and R.F. Reitemeier, *J. Phys. Chem.*, 39, 593–604, 1935.
112. A. Kahn, *J. Colloid Interf. Sci.*, 13, 51–60, 1958.
113. A.K. Helmy and E.A. Ferreiro, *Electroanal. Chem. Interf. Electrochem.*, 57, 103–112, 1974.
114. H.S. Arora and N.T. Coleman, *Soil Sci.*, 127, 134–139, 1979.
115. E. Frey and G. Lagaly, *J. Colloid Interf. Sci.*, 70, 46–55, 1979.
116. J.D. Oster, I. Shainberg, and J.D. Wood, *Soil Sci. Soc. Am. J.*, 44, 955–959, 1980.
117. R. Keren, I. Shainberg, and E Klein, *Soil Sci. Soc. Am. J.*, 52, 76–80, 1988.
118. S. Goldberg and H.S. Forster, *Soil Sci. Soc. Am. J.*, 54, 714–718, 1990.
119. R. Perkins, R. Brace, and E. Matijević, *J. Colloid Interf. Sci.*, 48, 417–426, 1974.
120. T. Permien and G. Lagaly, *J. Colloid Polym. Sci.*, 272, 1306–1312, 1994.
121. T. Permien, G. Lagaly, *Clays Clay Miner.*, 43, 229–236, 1995.
122. H. Heller and R. Keren, Clays Clay Miner., 49, 286–291, 2001.
123. G. Lagaly, O. Schulz, and R. Zimehl, *Dispersionen und Emulsionen. Eine Einführung in die Kolloidik feinverteilter Stoffe einschließlich der Tonminerale*, Mit einem historischen Beitrag über Kolloidwissenschaftler von Klaus Beneke, Steinkopff Verlag, Darmstadt, 1997, pp. 1–560.
124. D. Penner and G. Lagaly, *Clays Clay Miner.*, 48, 246–255, 2000.
125. D. Penner and G. Lagaly, *Appl. Clay Sci.*, 19, 131–142, 2001.
126. W. Stumm, C.P. Huang, and S.R. Jenkins, *Croatia Chem. Acta.*, 42, 233–244, 1970.
127. J.N. de Rooy, P.L. de Bruyn, and J.T.G. Overbeek, *J. Colloid Interf. Sci.*, 75, 542–554, 1980.
128. S.D. Lubetkin, S.R. Middleton, and R.H. Ottewill, *Philos. Trans. R. Soc., London, A*, 311, 353–368, 1984.

129. E, Tombácz, I, Abrahám, M, Gilde, and F. Szántó, *Colloids Surf.*, 49, 71–80, 1990.
130. R.O. James and G.A. Parks, in *Surface and Colloid Science*, Vol. 12, E. Matijević, Ed., Plenum Press, New York, 1982, p. 119.
131. J.A. Davies, R.O. James, and J.O. Leckie, *J. Colloid Interf. Sci.*, 63, 480–499, 1978.
132. S.E. Miller and P.F. Low, *Langmuir*, 6, 572–578, 1990.
133. J.P. Quirk and S. Marčelja, *Langmuir*, 13, 6241–6248, 1997.
134. R.M. Pashley and J.P. Quirk, *Colloids Surf.*, 9, 1–17, 1984.
135. E. Frey and G. Lagaly, Proceedings of the International Clay Conference, Oxford, 1978, M. Mortland and V.C. Farmer, Eds., Elsevier, Amsterdam, 1979, pp. 131–140.
136. G. Lagaly, G. Schön, and A.Weiss, *Kolloid Z. Z. Polym.*, 250, 667–674, 1972.
137. B.V. Derjaguin, N.V. Churaev, and V.M. Müller, *Surface Forces*, Consultants Bureau, New York, 1987
138. R.J. Pugh and J.A. Kitchener, *J. Colloid Interf. Sci.*, 35, 636–664, 1971.
139. P. Nadeau, *Appl. Clay Sci.*, 2, 83–93, 1987.
140. G. Lagaly, in Lectures Conferencias, Euroclay '87, J.L. Pérez-Rodriguez and E. Galan, Eds., Sociedad Espanola de Arcillas, Sevilla, 1987, pp. 97–115.
141. T. Stutzmann and B. Siffert, *Clays Clay Miner.*, 25, 392–406, 1977.
142. J.Y. Bottero, M. Bruant, J.M. Cases, D. Canet, and F. Fiessinger, *J. Colloid Interf. Sci.*, 124, 515–527, 1988.
143. A.F. Hollander, P. Somasundaran, and C.C. Gryte, in *Adsorption from Aqueous Solution*, P.H. Tewari, Ed., Plenum Press, New York, 1981, pp. 143–162.
144. E. Pefferkorn, I. Nabzar, and A. Carroy, *J. Colloid Interf. Sci.*, 106, 94–103, 1985.
145. L. Nabzar and E. Pefferkorn, *J. Colloid Interf. Sci.*, 108, 243–248, 1985.
146. E. Pefferkorn, L. Nabzar, and R. Varoqui, *Colloid Polym. Sci.*, 265, 889–896, 1987.
147. P. Stenius, L. Järnström, and M. Rigdahl, *Colloids Surf.*, 51, 219–238, 1990.
148. L. Nabzar, E. Pefferkorn, and R. Varoqui, *J. Colloid Interf. Sci.*, 102, 380–388, 1984.
149. L.T. Lee, R. Rahbari, J. Lecourtier, and G. Chauveteau, *J. Colloid Interf. Sci.*, 147, 351–357, 1991.

150. H.S. Kim, C. Lamarche, and A. Verdier, *Colloid Polym. Sci.*, 261, 64–69, 198.
151. G. Durand-Piana, F. Lafuma, and R. Audebert, *J. Colloid Interf. Sci.*, 119, 474–480, 1987.
152. N. Larsson and B Siffert, *J. Colloid Interf. Sci.*, 93, 424–431, 1983.
153. C. Breen, J.O. Rawson, and B.E. Mann, *J. Mater. Chem.*, 6, 253–260, 1996.
154. J. Billingham, C. Breen, J.O. Rawson, J. Yarwood, and B.E. Mann, *J. Colloid Interf. Sci.*, 193, 183–189, 1997.
155. D.P. Parazak, C.W. Burkhardt, K.J. McCarthy, and M.P. Stehlin, *J. Colloid Interf. Sci.*, 123, 59–72, 1988.
156. H. Xiao, Z. Lui, and N. Wiseman, *J. Colloid Interf. Sci.*, 216, 409–417, 1999.
157. B. Alince, F. Bednar, and T.G.M. van de Ven, *Colloids Surf. A,* 190, 71–81, 2001.
158. U. Hofmann, *Ber. Dtsch. Keram. Ges.*, 38, 201–207, 1961.
159. U. Hofmann, *Keram. Z.*, 14, 14–19, 1962.
160. U. Hofmann, *Ber. Dtsch. Keram. Ges.*, 41, 680–686, 1964.
161. T. Permien and G. Lagaly, *Clay Miner.*, 29, 751–760, 1994.
162. A. Weiss and R. Frank, *Z. Naturforsch.*, 16b, 141–142, 1961.
163. A. Weiss, *Rheologica Acta*, 2, 292–304, 1962.
164. E. Tombácz, I. Balázs, J. Lakatos, and F. Szántó, *Colloid Polym. Sci.*, 267, 1016–1025, 1989.
165. I. Lapides and L. Heller-Kallai, *Colloid Polym. Sci.*, 280, 554–561, 2002.
166. J.M. Benna, N. Kbir-Ariguib, C. Clinard, and F. Bergaya, *Prog. Colloid Polym. Sci.*, 117, 204–210, 2001.
167. J.M. Benna, N. Kbir-Ariguib, C. Clinard, and F. Bergaya, *Appl. Clay Sci.*, 19, 103–120, 2001.
168. S. Abend and G. Lagaly, *Appl. Clay Sci.*, 16, 201–227, 2000.
169. N. Güven and R.M. Pollastro, Eds., *Clay–water Interface and its Rheological Implications*, CMS Workshop Lectures, Vol. 4, The Clay Minerals Society, Boulder, CO, USA, 1992, pp. 1–244.
170. Y. Adachi, K. Nakaishi, and M. Tamak, *J. Colloid Interf. Sci.*, 198, 100–105, 1998.
171. C.H. Pons, F. Rousseaux, and D. Tschoubar, *Clay Miner.*, 16, 23–42, 1981.
172. F. Hetzel, D. Tessier, A.M. Jaunet, and H. Doner, *Clays Clay Miner.*, 42, 242–248, 1994.

173. K. Faisander, C.H. Pons, D. Tchoubar, and F. Thomas, *Clays Clay Miner.*, 46, 636–648, 1998.
174. G.F. Walker, *Nature*, 187, 312, 1960.
175. W.G. Garett and G.F. Walker, *Clays Clay Miner.*, 9, 557–567, 1962.
176. J.A. Rausell-Colom, *Trans. Faraday Soc.*, 60, 190–201, 1964.
177. M.V. Smalley, R.K. Thomas, L.F. Braganza, and T. Matsuo, *Clays Clay Miner.*, 37, 474–478, 1989.
178. L.F. Braganza, R.J. Crawford, M.V. Smalley, and R.K. Thomas, *Clays Clay Miner.*, 38, 90–96, 1990.
179. H.L.M. Hatharasinghe, M.V. Smalley, J. Swenson, A.C. Hannon, and S.M. King, *Langmuir*, 16, 5562–5567, 2000.
180. M.V. Smalley, H.L.M. Hathrasinghe, I. Osborne, J. Swenson, and S. King, *Langmuir*, 17, 3800–3812, 2001.
181. G. Lagaly, in *Interaction of Water in Ionic and Nonionic Hydrates*, H. Kleeberg, Ed., Springer-Verlag, Berlin, 1987, pp. 229–240.
182. M.V. Smalley, *Langmuir*, 10, 2884–2891, 1994.
183. M.V. Smalley, *Prog. Colloid Polym. Sci.*, 97, 59–64, 1994.
184. J.A. Rausell-Colom and P.S. Salvador, *Clay Miner.*, 9, 139–149, 1971.
185. J.A. Rausell-Colom and P.S. Salvador, *Clay Miner.*, 9, 193–208, 1971.
186. J.A. Rausell-Colom, J. Saez-Aunion, and C.H. Pons, *Clay Miner.*, 24, 459–478, 1989.
187. T.R. Jones, *Clay Miner.*, 18, 399–410, 1983.
188. W.T. Granquist and J. McAtee, *J. Colloid Sci.*, 18, 409–420, 1963.
189. V.N. Moraru, *Appl. Clay Sci.*, 19, 11–26, 2001.
190. B. Gherardi, A. Tahani, P. Levitz, and F. Bergaya, *Appl. Clay Sci.*, 11, 163–170, 1996.